Methane sources and sinks in Lake Kivu

Natacha Pasche,[1,2,3] Martin Schmid,[1] Francisco Vazquez,[1] Carsten J. Schubert,[1] Alfred Wüest,[1,2] John D. Kessler,[4] Mary A. Pack,[5] William S. Reeburgh,[5] and Helmut Bürgmann[1]

Received 17 February 2011; revised 8 April 2011; accepted 21 April 2011; published 22 July 2011.

[1] Unique worldwide, Lake Kivu stores enormous amounts of CH_4 and CO_2. A recent study reported that CH_4 concentrations in the lake have increased by up to 15% in the last 30 years and that accumulation at this rate could lead to catastrophic outgassing by ~2100. This study investigates the present-day CH_4 formation and oxidation in Lake Kivu. Analyses of ^{14}C and ^{13}C in CH_4 and potential carbon sources revealed that below 260 m, an unusually high ~65% of the CH_4 originates either from reduction of geogenic CO_2 with mostly geogenic H_2 or from direct inflows of geogenic CH_4. Aerobic CH_4 oxidation, performed by close relatives of type X CH_4-oxidizing bacteria, is the main process preventing CH_4 from escaping to the atmosphere. Anaerobic CH_4 oxidation, carried out by CH_4-oxidizing archaea in the SO_4^{2-}-reducing zone, was also detected but is limited by the availability of sulfate. Changes in $^{14}C_{CH4}$ and $^{13}C_{CH4}$ since the 1970s suggest that the amount of CH_4 produced from degrading organic material has increased due to higher accumulation of organic matter. This, as well as the sudden onset of carbonates in the 1960s, has previously been explained by three environmental changes: (1) introduction of nonnative fish, (2) amplified subaquatic inflows following hydrological changes, and (3) increased external inputs due to the fast growing population. The resulting enhancement of primary production and organic matter sedimentation likely caused CH_4 to increase. However, given the large proportion of old CH_4 carbon, we cannot exclude an increased inflow of geogenic H_2 or CH_4.

Citation: Pasche, N., M. Schmid, F. Vazquez, C. J. Schubert, A. Wüest, J. D. Kessler, M. A. Pack, W. S. Reeburgh, and H. Bürgmann (2011), Methane sources and sinks in Lake Kivu, *J. Geophys. Res.*, *116*, G03006, doi:10.1029/2011JG001690.

1. Introduction

[2] Methane (CH_4) and carbon dioxide (CO_2) are major end products of organic matter decomposition in water bodies. In lacustrine sediments, the most important CH_4-producing pathways are acetoclastic methanogenesis and CO_2 reduction [*Conrad*, 2005]:

$$CH_3COOH \rightarrow CO_2 + CH_4 \quad (1)$$

$$CO_2 + 4H_2 \rightarrow CH_4 + 2H_2O. \quad (2)$$

Once produced, CH_4 can be oxidized either in the sediment, at the sediment-water interface, or in the open water, depending on the availability of oxidants. Two different biological processes are currently considered to be the main contributors to CH_4 oxidation in aquatic systems: oxidation by aerobic methanotrophic bacteria and anaerobic CH_4 oxidation by syntrophic consortia of CH_4-oxidizing archaea and SO_4^{2-}-reducing bacteria [*Hinrichs and Boetius*, 2002; *Schubert et al.*, 2010]. CH_4 that is not consumed is eventually transported to shallower waters and can be released to the atmosphere where it acts as a potent greenhouse gas. It has been estimated that lakes contribute 6 to 16% to global CH_4 emissions to the atmosphere [*Bastviken et al.*, 2004]. CH_4 oxidation therefore plays an important role in controlling lacustrine CH_4 emissions.

[3] Lake Kivu is an African Rift lake (Figure 1) with a permanently stratified hypolimnion that contains an estimated 60 km^3 of CH_4 and 300 km^3 of CO_2 (gas volume at 0°C and 1 atm [*Schmid et al.*, 2005]). CH_4 accumulation in the lake bears the risk of catastrophic outgassing similar to the limnic eruptions in Lakes Nyos [*Kling et al.*, 1987] and Monoun [*Sigurdsson et al.*, 1987]. Conversely, extraction of the lake's CH_4 could provide enough energy to supply the lake's bordering countries with electricity for a decade [*Jones*, 2003]. The origin of these gases, however, has been a matter of controversy [*Deuser et al.*, 1973; *Tietze et al.*, 1980]. Most authors agree that the CO_2 has a primarily geogenic origin, whereas the CH_4 is biogenic [*Schoell et al.*,

[1]Eawag: Swiss Federal Institute of Aquatic Science and Technology, Surface Waters—Research and Management, Kastanienbaum, Switzerland.
[2]Institute of Biogeochemistry and Pollutant Dynamics, Swiss Federal Institute of Technology, Zürich, Switzerland.
[3]Now at Lake Kivu Monitoring Program, Ministry of Infrastructure, Gisenyi, Rwanda.
[4]Department of Oceanography, Texas A&M University, College Station, Texas, USA.
[5]Department of Earth System Science, University of California, Irvine, California, USA.

0148-0227/11/2011JG001690

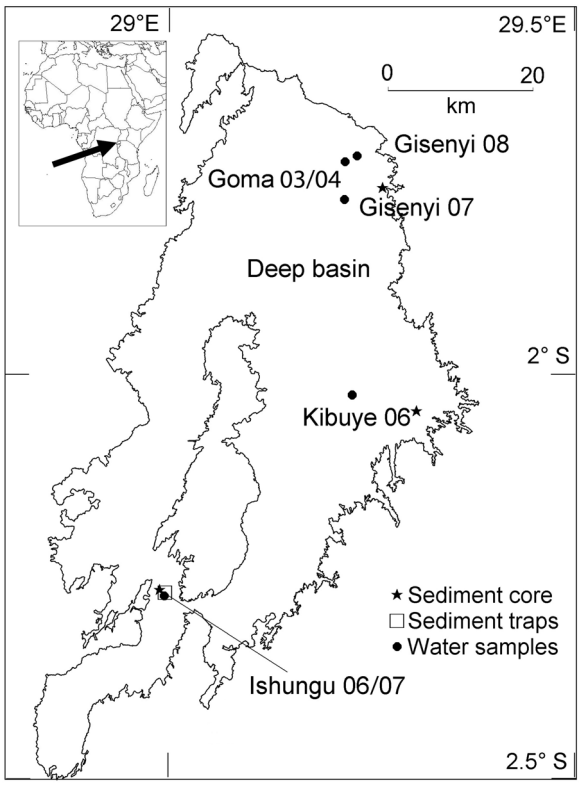

Figure 1. Map of Lake Kivu showing the locations of water sampling, sediment cores, and the mooring with sediment traps. In the deep basin, the names of the sampling locations (Goma 03/04 (6–11 November 2003; 26 February 2004), Kibuye 06 (5 May 2006), Gisenyi 07 (12 May 2007), Gisenyi 08 (October 2008)) represent the nearest city followed by the sampling year. In Ishungu Basin, water samples (17 May 2007) were taken at the same site Ishungu 06/07 as the sediment traps (17 May 2006 to 7 January 2008) and the sediment core (14 May 2006).

1988; *Tietze*, 1978; *Tietze et al.*, 1980]. *Schoell et al.* [1988] reported that two thirds of CH_4 is produced by reduction of geogenic CO_2 and one third by acetoclastic methanogenesis of sedimentary organic material (biogenic material).

[4] Based on CH_4 concentrations observed by *Tietze* [1978] and recent measurements, *Schmid et al.* [2005] estimated that CH_4 concentrations in the lake may have increased by up to 15% over the last 30 years. An increase in CH_4 formation by about a factor of 3 compared to the long-term steady state formation would have been required to explain this increase. A recent study further provided evidence that Lake Kivu experienced an increase in gross and organic carbon (OC) sedimentation since the 1960s due to (1) a modified internal food web following the introduction of the nonnative Tanganyika sardine (*Limnothrissa miodon*); (2) hydrological changes that enhanced internal upwelling; and/or (3) increased external nutrient inputs caused by the fast growing human population [*Pasche et al.*, 2010]. We hypothesize that the increase in OC sedimentation is partly responsible for the increasing CH_4 concentrations in the lake. Since the risk of outgassing increases with rising gas content, our main research interest is to understand the driving forces of CH_4 formation and consumption. Further, the CH_4 formation rate is of practical interest for planning the forthcoming exploitation of CH_4.

[5] This study is part of a larger project that assessed the nutrient cycling and its relation to CH_4 in Lake Kivu. Analyses of the external inputs [*Muvundja et al.*, 2009] and the internal loading [*Pasche et al.*, 2009] of nutrients highlighted the importance of the lake internal processes for the nutrient cycling in the lake. Observations from sediment cores indicated recent changes in the nutrient cycling that might be related to the observed increase in CH_4 concentrations [*Pasche et al.*, 2010]. In the present study, the lessons learned from the analysis of the nutrient fluxes are combined with (1) measurements of the isotopic composition of different carbon pools and (2) the analysis of the microbial community in the water column, for the following three objectives: (1) to assess the rates of CH_4 formation through acetoclastic methanogenesis and CO_2 reduction; (2) to determine aerobic and anaerobic CH_4 oxidation rates and the organisms involved; and (3) to detect changes in the carbon fluxes which could explain the recent CH_4 increase.

2. Site Description

[6] Lake Kivu is located in the East African Rift Valley, between the Republic of Rwanda and the Democratic Republic of the Congo. At an elevation of 1463 m, it has an area of 2370 km^2, a volume of 580 km^3 and a maximum depth of 485 m [*Schmid et al.*, 2004; *Tietze*, 1978]. The lake is meromictic and the mesotrophic epilimnion is permanently separated from the anoxic nutrient-rich deep waters. The depth of the oxycline varies seasonally from 30 m during the rainy season (October to May) to 60–65 m in the windy dry season (June to September). The permanently stratified deep water is further characterized by a major chemocline extending from 255 to 262 m. Subaquatic springs enter the permanently stratified deep water at different depths, with an estimated total inflow of ~1.3 $km^3\ yr^{-1}$ [*Schmid et al.*, 2005]. More than 127 rivers with a total flow of ~2.4 $km^3\ yr^{-1}$ enter the lake from the catchment (5097 km^2), and 3.6 $km^3\ yr^{-1}$ flow out with the Ruzizi River [*Muvundja et al.*, 2009]. Precipitation (3.3 $km^3\ yr^{-1}$) is nearly equal to lake surface evaporation (3.4 $km^3\ yr^{-1}$) [*Muvundja et al.*, 2009].

[7] Water residence times in the permanently stratified deep water are two to three orders of magnitude longer than time scales for horizontal mixing. Physical and chemical properties are therefore horizontally homogeneous throughout the lake, except for the separate basins of Kabuno Bay and Bukavu Bay. Energy supply from the wind to the deep water is limited by the strong density stratification in the lake. Consequently vertical exchange by turbulent diffusivity is weak, as evidenced by the presence of double-diffusive staircases [*Schmid et al.*, 2010]. Vertical transport is therefore dominated by the upwelling caused by the inflows of the subaquatic springs. Water below the major chemocline has a residence time of 800 to 1,000 years, which has led to an enormous accumulation of dissolved gases and nutrients [*Schmid et al.*, 2005].

[8] Nutrients for primary production are supplied to the productive surface layer mainly by internal recycling by upwelling from the nutrient-rich deep waters [*Pasche et al.*, 2009]. Contrary to many other large lakes, such as Tanganyika, where

nutrient supply by upwelling at the southern end leads to horizontal gradients in primary production [*Bergamino et al.*, 2010], the internal recycling in Lake Kivu is homogeneous, as indicated by the perfectly horizontal layering. Consequently, low spatial variability of primary production and chlorophyll concentrations have been observed in the surface waters of the lake [*Kneubühler et al.*, 2007; *Sarmento et al.*, 2009].

3. Material and Methods

3.1. Sampling

[9] Sampling was conducted during five field campaigns in November 2003, February 2004 (site Goma 03/04), May 2006 (Kibuye 06), May 2007 (Gisenyi 07) and October 2008 (Gisenyi 08) at three different locations in the main basin (Figure 1). In May 2006 and 2007 samples were taken in the Ishungu Basin (site Ishungu 06/07, Figure 1). Water samples were collected using 5 L Niskin bottles. For depths below 200 m, the open top valve was capped with a balloon to prevent sample loss due to vigorous outgassing during bottle ascent.

[10] Gas samples were obtained using a new device consisting of a 500 mL metal cylinder for water sampling and an evacuated 250 mL metal cylinder to collect the gases. These collected gases were subsampled into evacuated 120 mL airtight glass vials.

[11] The sampling of sediment traps and cores has been described in detail by *Pasche et al.* [2010]. In May 2007, a sediment core for gas analysis was taken near Gisenyi (1°46.416′S, 29°15.796′E, 125 m depth) using an Uwitec gravity corer. Thirteen sediment samples (2 mL) were extracted between 0 and 16 cm through side ports using plastic syringes. They were transferred to 25 mL glass vials prefilled with 4 mL of 2.5% sodium hydroxide (NaOH) [*Sobek et al.*, 2009]. The vials were immediately sealed with butyl-rubber stoppers, shaken, and stored upside down until analysis for CH_4 concentration and isotopic composition. Further gravity sediment cores were taken in May 2006 at Ishungu (2°16.077′S, 28°59.374′E, 175 m depth) for total organic carbon (TOC) analyses and at Kibuye (2°02.886′S, 29°18.307′E, 190 m depth) for TOC and ^{13}C and ^{14}C analyses of the OC.

[12] A sediment trap mooring was set in Ishungu Basin from May 2006 to January 2008 (Ishungu 06/07). Sediment traps consisting of two plastic cylinders (diameter 9.2 cm, length 100 cm) were placed at four different depths (50, 90, 130 and 172 m). Trap material without any poisoning was collected monthly with overlying water in 250 mL bottles, frozen and transported to Switzerland.

3.2. Chemical Parameters

[13] In October 2008, water samples for the analyses of organic anions were taken at site Gisenyi 08 (Figure 1). Samples were preserved in the field by adding 10 M NaOH to adjust the pH to 12. Organic anions (lactate, acetate, propionate, formate, butyrate, pyruvate) were measured with a Dionex DX-320 ion chromatography system with a detection limit of 5 μmol L^{-1}. For TOC measurements, water samples were collected in 200 mL glass vials and acidified to pH 3 to remove inorganic carbon. TOC was measured within 6 days with a Total Organic Carbon Analyzer (Shimadzu TOC-V CPH).

[14] For CH_4 concentrations and isotopic ratio analyses, water samples were taken in 2006 and 2007 at sites Kibuye 06, Ishungu 06/07 and Gisenyi 07 (Figure 1) and for CO_2 isotopic ratio analyses in 2003 at site Goma 03/04. Samples were transferred to 120 mL glass vials and poisoned with cupric chloride ($CuCl_2$). All samples were measured within five weeks of collection. CH_4 concentrations were measured by a headspace (30 mL N_2) technique similar to that of *McAuliffe* [1971]. CH_4 concentrations were determined on a gas chromatograph (Agilent, 6890) equipped with a Carboxen 1010 column (30 m, Supelco) using a flame ionization detector. In order to dilute samples from below 70 m depth into the calibration range of the GC, 300 μL of headspace were transferred into 58.5 mL serum vials prefilled with N_2. Dissolved gas concentrations were calculated after *Wiesenburg and Guinasso* [1979], including the effects of salinity.

[15] Methane carbon isotopes ($^{13}C_{CH4}$) were determined using the method of *Sansone et al.* [1997]. Duplicate measurements were processed with an IsoPrime mass spectrometer connected to a trace gas preconcentrator (GV Instruments). Results are noted in the standard δ notation relative to Vienna Pee Dee Belemnite.

[16] Carbon isotopes on carbon dioxide ($^{13}C_{CO2}$) were determined using an IsoPrime mass spectrometer connected to a trace gas preconcentrator (GV Instruments). Results are noted in the standard δ notation relative to Vienna Pee Dee Belemnite.

[17] Methane radiocarbon ($^{14}C_{CH4}$), deuterium ($^{2}H_{CH4}$), and stable carbon isotope ($^{13}C_{CH4}$) analyses were performed on samples taken in 2007, at site Gisenyi 07. The methods are outlined in *Kessler and Reeburgh* [2005]. Briefly, CH_4 was extracted from samples, purified, and combusted to CO_2 and water. An aliquot of CO_2 was converted to elemental carbon by iron-catalyzed hydrogen reduction and analyzed with ^{14}C Accelerator Mass Spectrometer (AMS) at the Keck Carbon Cycle AMS Facility. ^{14}C concentrations are given as percent of the modern standard (percent modern carbon, pMC) following the conventions of *Stuiver and Polach* [1977]. A second aliquot of CO_2 was analyzed for ^{13}C by dual-inlet isotope ratio mass spectrometry at the University of California Irvine (UCI) Stable Isotope Facility. The water produced from CH_4 combustion was reduced to hydrogen with activated zinc and the $^{2}H_{CH4}$ was measured on a Finnigan MAT 252 Mass Spectrometer at UCI and is reported in delta notation relative to Standard Mean Ocean Water. The ^{14}C content of the organic matter in three samples from the Kibuye sediment core (0–0.5 cm, 0–5 cm, 15–37 cm), was measured in the Laboratory of Ion Beam Physics at the Swiss Federal Institute of Technology (ETH) in Zurich using the method described by *Hajdas et al.* [1993].

[18] For TOC in sediment, total carbon (TC) was measured using a combustion CNS elemental analyzer (VARIO Co and EuroVector Co). Total inorganic carbon (TIC) was analyzed as CO_2 by coulometry (UIC Coulometrics) after acidification with 3M hydrochloric acid (HCl). TOC was calculated as the difference between TC and TIC.

3.3. Methane Oxidation Measurements

[19] To experimentally verify CH_4 oxidation, CH_4 concentrations were monitored in vials over 5 days in 2007. At site Gisenyi 07, water from 20, 40, 60, 80, and 100 m depth

Table 1. Primers and Methods Used for PCR Amplification

Gene	Primer	Target Group	Analysis/Screening	Reference
16S rRNA	341f[a]-534r	Bacteria	DGGE, direct seq.	1
pmoA	A189f[a]-A650r	aerobic methanotrophs	DGGE, cloning and seq.	2 and 3
mcrA	Me1f-Me2r	anaerobic methanotrophs/methanogens	RFLP, cloning and seq.	2 and 4

[a]Primer also used with GC clamp [*Muyzer et al.*, 1993] for DGGE; seq., 16S rRNA DGGE bands were sequenced directly, *pmoA* and *mcrA* were cloned and screened using the given method before sequencing. See section 3. References are 1, *Muyzer et al.* [1993]; 2, *Earl et al.* [2003]; 3, *Bourne et al.* [2001]; and 4, *Hales et al.* [1996].

was sampled in five 120 mL airtight vials for each depth (Table 1). One bottle was poisoned with $HgCl_2$ immediately after sampling and then for the following four days one vial per day was poisoned and analyzed as above. For the samples from 20, 40, and 60 m depth CH_4 was further analyzed for ^{13}C on day one and day five.

3.4. Microbial Community Analysis

3.4.1. Molecular Analyses

[20] During May 2007, water samples (380 to 750 mL) from 14 depths collected at Gisenyi 07 were filtered through polycarbonate filters (0.2 μm, 47 mm). DNA was extracted from the filters as described by *Llirós et al.* [2008]. The bacterial community structure was investigated by Polymerase Chain Reaction (PCR) amplification of the partial 16S ribosomal RNA gene with primers 341f-GC and 534r (Table 1) followed by denaturing gradient gel electrophoresis (DGGE) [*Muyzer et al.*, 1993]. Selected bands were cut from the gel, reamplified, and sequenced. The particulate CH_4 monooxygenase gene (*pmoA*) served as a molecular marker for aerobic methanotrophs; *pmoA* was detected by PCR amplification with *pmoA*-specific primers A189f and A650r (Table 1) as described by *Bourne et al.* [2001] with minor modifications. As a marker for anaerobic methanotrophs (ANME) as well as methanogens, the gene for methyl coenzyme M reductase (*mcrA*) was amplified using *mcrA*-specific primers Me1f and Me2r [*Hales et al.*, 1996] (Table 1); *mcrA* genetic diversity was characterized by restriction fragment length polymorphism analysis (RFLP) [*Earl et al.*, 2003]. Clone libraries were created from amplicons from seven depths for *mcrA* and three depths for *pmoA*. Clones were screened using DGGE (*pmoA*) and RFLP (*mcrA*) and selected clones were commercially sequenced (Microsynth, Balgach, Switzerland). Sequences were submitted to the GenBank nucleotide sequence database with the following accession numbers: 16*S rRNA*, FJ952083 to FJ952140; *pmoA*, FJ952083 to FJ952102; *mcrA*, FJ952103 to FJ952140. Detailed protocols are presented in Text S1 in the auxiliary material.[1]

3.4.2. Analysis of Sequenced Data

[21] Sequences were screened, trimmed, aligned (using Clustal W [*Larkin et al.*, 2007]) and analyzed using Mega 4.1 software [*Tamura et al.*, 2007]. Reference sequences were retrieved using the BLAST network services [*Altschul et al.*, 1990] and keyword queries of the nucleotide database at the National Center for Biotechnology Information using the Entrez Database Query Tool (http://www.ncbi.nlm.nih.gov/nuccore). General bacterial 16S rRNA sequences from DGGE bands were classified using the Classifier Tool on the Ribosomal Database Project 2 Web site (http://rdp.cme.msu.edu/; release 10 [*Wang et al.*, 2007]). Phylogenetic trees for *mcrA* and *pmoA* were constructed based on translated amino acid sequences using the unweighted pair group method with arithmetic mean (UPGMA) hierarchical clustering method [*Nei and Kumar*, 2000] and the PAM distance metric [*Schwarz and Dayhoff*, 1979] as implemented in Mega 4.1, with pairwise elimination of gaps and 1000 bootstrap resamplings for tree testing.

4. Results

4.1. Chemistry of the Water Column

[22] Lake Kivu is characterized by high amounts of dissolved gases, with CO_2 concentrations five times higher than CH_4 (Figure 2a). Gas concentrations rise gradually with depth down to the major chemocline (255 to 262 m) where they abruptly increase. Gas concentrations measured in water samples compare well with published data [*Schmid et al.*, 2005] above 140 m (Figure 3c). However, below 140 m, part of the CH_4 was lost due to vigorous outgassing during sampling.

[23] The profiles of the main electron acceptors (O_2, SO_4^{2-}, and NO_3^-) indicated a typical succession of redox zones for stratified water bodies (Figure 2b) and were described in detail by *Pasche et al.* [2009]. The oxycline extended to a depth of 50 m in May 2006 and 2007. Below the oxycline, SO_4^{2-} decreased with a sharp gradient to 80 m and dropped below detection (0.05 mmol L^{-1}) at 100 m depth. In contrast, H_2S was absent above the oxycline, increased sharply between 50 and 80 m depth, and more gradually to 150 m. Below 150 m H_2S remained constant at ~0.27 mmol L^{-1} (data not shown). Other electron acceptors, namely NO_3^-, manganese (see the reduced product Mn^{2+}, Figure 2b) and Fe (III) (not shown) were present only in very low concentrations.

[24] TOC concentrations increased from 1.8 mg L^{-1} at 40 m to 4.2 mg L^{-1} at 360 m depth. Acetate and other short-chain organic anions were below the detection limit of 5 μmol L^{-1}.

4.2. Methane and Carbon Isotopic Signature

4.2.1. Water Column

[25] Above 90 m, $\delta^{13}C_{CH4}$ increased from −59.8‰ to −43‰ at the surface, with a high variability within and above the oxycline (Figure 3a). Below 90 m, $\delta^{13}C_{CH4}$ was constant at −59.8 ± 1‰. $\delta^{2}H_{CH4}$ below 140 m averaged at −215‰, with a considerable error margin. Values decreased in excess of the error between 140 m and 255 m. The decrease in the water column above the chemocline is supported by two separate measurements analyzed in a different laboratory (Figure 3b, open circles). A sharp increase in excess of the error was observed at the main chemocline. Below the

[1]Auxiliary materials are available in the HTML. doi:10.1029/2011JG001690.

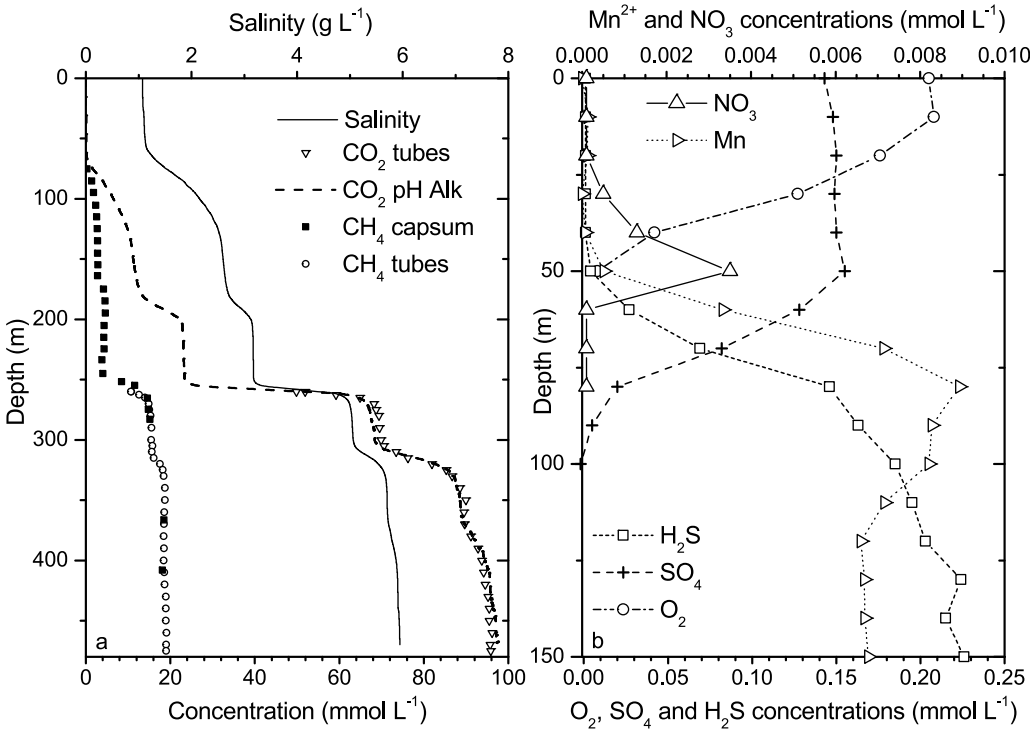

Figure 2. (a) Vertical profiles of salinity and concentrations of dissolved gases (sampled 2003 at site Goma 03/04) in Lake Kivu from *Schmid et al.* [2005]. The dashed curve is the CO_2 concentration calculated from pH and alkalinity. CO_2 was measured by slowly pumping water in polyethylene tubes and analyzing the gas and liquid flows. CH_4 concentrations [*Schmid et al.*, 2005] were measured in situ with a Capsum Mets sensor and on a platform using polyethylene tubes (see above). The salinity profile was calculated from a conductivity profile measured with a conductivity-temperature-depth (CTD) probe. (b) Top 150 m of vertical profiles of electron acceptors concentrations O_2, NO_3^-, SO_4^{2-} from *Pasche et al.* [2009] and reduced species Mn^{2+} and H_2S. These profiles are the average of three stations in the deep basin and two observations in Ishungu Basin taken in February 2004, May 2006, and May 2007.

chemocline, δ^2H_{CH4} decreased again to an average of −220‰ (Figure 3b). pMC decreased from 15.7% at 140 m depth to 12.9% at 250 m depth. Across the chemocline it decreased steeply to 11.9% at 255 m and 11.1% at 270 m. Below the chemocline pMC increased slightly to 11.6% at 440 m. Conversion to ^{14}C age [*Stuiver and Polach*, 1977] indicates an average age of 17,000 years for CH_4 (Figure 3b). In comparison, the residence time of water below 250 m has been estimated to be ~800 years [*Schmid et al.*, 2005], indicating the strong influence of geogenic CO_2 with a dead radiocarbon signal.

4.2.2. Sediment

[26] The $\delta^{13}C_{CH4}$ measured in the Gisenyi core decreased slightly from the surface (−66‰) to a minimum of −68‰ at 15 cm depth (Figure 4).

[27] In the Kibuye core, representing the last 300 years [*Pasche et al.*, 2010], isotope signatures of OC ($\delta^{13}C_{OC}$) varied slightly around −24.1‰ (−22.6 to −25.1‰). The ^{14}C content of OC ($^{14}C_{OC}$) in this core varied with depth. In the top layer (0–0.5 cm, last 2–3 years) it was 34 pMC (carbon age 8,670 years), a mixed sample of the section including the bomb peak (0.5–5 cm, last 20 years) had 43 pMC (6,780 years), while a mixed sample from before the bomb peak (15 to 37 cm, approximately representing the time between 300 and 100 years before present) was 28 pMC (10,200 years). The latter sample was assumed to be representative for the source organic matter in the sediment before the impact of bomb tests.

4.3. Estimating CH_4, CO_2, and Organic Carbon Fluxes

[28] In this section, the knowledge gained from previous studies is combined with the results of our measurements and model simulations described in the auxiliary material to create an overview of CH_4, CO_2, and OC fluxes in Lake Kivu. Error margins are calculated based on estimated error ranges for the measured quantities and standard formulas for error propagation. The fluxes estimated in the following sections are summarized in Figure 5.

4.3.1. Primary Production and CO_2 Fluxes

[29] Annual primary production (averaged over 2.5 years) was determined to be PP = 228 g C m^{-2} yr^{-1}, by *Sarmento et al.* [2009]. The total upward fluxes of CO_2 (internal loading, IL) and dissolved inorganic carbon (DIC) through the chemocline were previously estimated at $IL_{CO2} = 126 \pm 25$ g C m^{-2} yr^{-1} and $IL_{DIC} = 335 \pm 67$ g C m^{-2} yr^{-1} [*Pasche et al.*, 2009]. Since PP < IL_{DIC}, the lake is a net source of CO_2. The ^{14}C content of the sediment (Section 4.2.2) suggests that primary production uses only approximately one third to one fourth of atmospheric CO_2 as a carbon source.

4.3.2. Organic Carbon Fluxes

[30] OC analyses from sediment traps deployed at three different depths in the Ishungu Basin over two years revealed

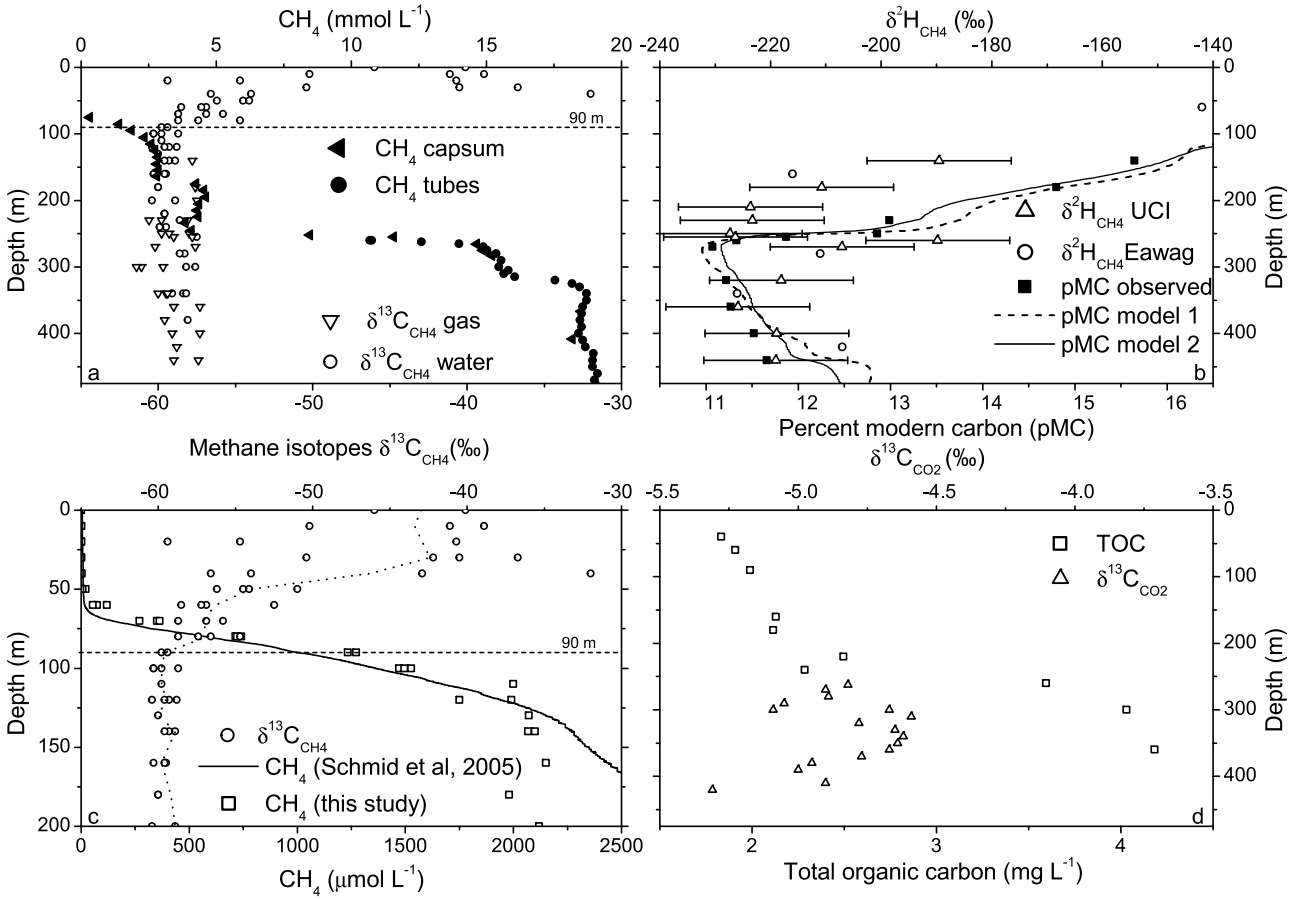

Figure 3. (a) Profiles of CH_4 concentrations [*Schmid et al.*, 2005] and ^{13}C isotopes (this study, data from samplings Kibuye 06, Ishungu 07, and Gisenyi 07). The $^{13}C_{CH4}$ was measured in gas and water samples collected during three field visits. Gas samples were fractionated by +0.7‰ compared to water samples. The dashed line represents the lower boundary of the SO_4^{2-}-reducing zone (90 m depth). (b) CH_4 deuterium isotopes (the large error bars of 13‰ represent the standard deviation of the standards, which were fractionated during sample preparation) and ^{14}C. The models used to reproduce the ^{14}C (given as percent modern carbon, pMC) depth profile (solid and dashed lines), are described in the auxiliary material. (c) Profiles between 0 and 200 m depth of CH_4 concentrations measured in this study (data from samplings Kibuye 06, Ishungu 07 and Gisenyi 07) compared with data from *Schmid et al.* [2005], as well as $\delta^{13}C_{CH4}$. The horizontal dashed line represents the lower limit of the SO_4^{2-}-reducing zone (90 m). The dotted curve is the averaged value for each depth of $\delta^{13}C_{CH4}$. (d) Profile of ^{13}C isotopes of dissolved CO_2 and total organic carbon (TOC) concentrations.

a homogeneous average gross sedimentation of $S_{OCgross}$ = 41 ± 2 g C m^{-2} yr^{-1} from 90 to 172 m depth [*Pasche et al.*, 2010]. However, comparisons with nutrient loading data and observations of phytoplankton abundance have shown that the observed gross sedimentation was approximately 60 ± 10% below the long-term average [*Pasche et al.*, 2010]. Thus, we estimate the long-term average of $S_{OCgross}$ to 110 ± 27 g C m^{-2} yr^{-1}. A sediment core taken at the same location revealed a net sedimentation of 7 g C m^{-2} yr^{-1} (top 10 cm, approx. 40 years). Higher values were found at Gisenyi (17 g C m^{-2} yr^{-1}) and Kibuye (13 g C m^{-2} yr^{-1}), providing a range of S_{OCnet} = 12 ± 5 g C m^{-2} yr^{-1} [*Pasche et al.*, 2010]. The mineralization rate of OC in the sediment was therefore estimated as

$$M_{OC\_sed} = S_{OCgross} - S_{OCnet} = 98 \pm 28 \text{ g C m}^{-2} \text{ yr}^{-1}.$$

4.3.3. Methane Fluxes From Organic Matter Decomposition in the Sediment

[31] Assuming methanogenesis proceeds to completion, the mineralized carbon partitions 1:1 between CO_2 and CH_4 [*Conrad*, 1999]. We can therefore calculate the total CH_4 formation (P_{CH4_sed}) based on the mineralization of the settling OC:

$$P_{CH4\_sed} = 0.5 \cdot M_{OC\_sed} = 49 \pm 14 \text{ g C m}^{-2} \text{ yr}^{-1}.$$

[32] Independently, the CH_4 flux from the sediment to the water column was calculated from CH_4 concentrations measured in the Gisenyi sediment core taken at 125 m water depth. Undisturbed cores could not be retrieved from greater depths, since outgassing destroyed the layering within the core. A net CH_4 flux from the sediment to the water column of

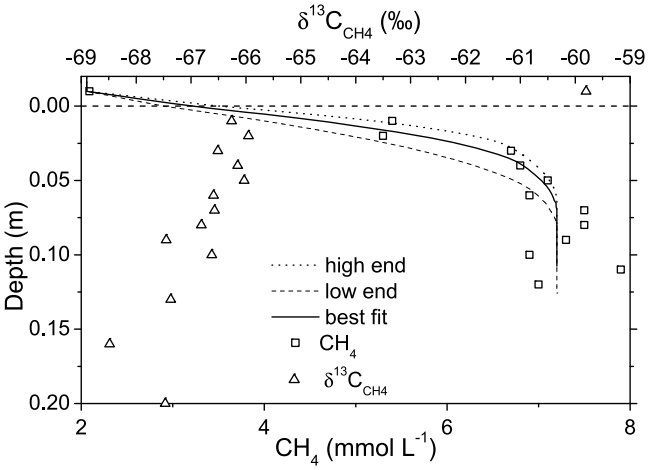

Figure 4. Profiles of CH_4 concentration and $^{13}C_{CH4}$ isotopes in the top sediment. The dashed line marks the sediment-water interface at 125 m depth. CH_4 concentration and isotope values in the water column at 125 m depth taken at a different location are plotted for comparison. The three lines, representing the best fit (solid curve, corresponding to a flux of ~80 g C_{CH4} m^{-2} yr^{-1}), the lower end (dashed curve, ~60 g C_{CH4} m^{-2} yr^{-1}), and the higher end (dotted curve, ~100 g C_{CH4} m^{-2} yr^{-1}), were determined with the one-dimensional diffusion-reaction model described by *Müller et al.* [2003].

60 to 100 g C_{CH4} m^{-2} yr^{-1} was estimated with the one-dimensional diffusion-reaction model described by *Müller et al.* [2003], by setting in situ CH_4 concentrations in the water column (2.1 mmol L^{-1}, measured at a different site) at 1 cm above the sediment. Due to uncertainty about the thickness of the diffusive boundary layer in Lake Kivu, these values are only a rough estimate based on reasonable assumptions. The upper estimate is well outside the possible rate of methanogenesis based on the reported organic matter deposition rate, but the lower estimate falls within the range for P_{CH4_sed} estimated above. The CO_2 flux is assumed to be equal to the CH_4 flux:

$$P_{CO2\_sed} = P_{CH4\_sed} = 49 \pm 14 \text{ g C } m^{-2} \text{ } yr^{-1}.$$

4.3.4. Partitioning Between CO_2 Reduction and Acetoclastic Methanogenesis

[33] In order to reproduce the $^{14}C_{CH4}$ vertical profile in the water column (Figure 3b), we used an extended version of the one-dimensional diffusion advection model described by *Schmid et al.* [2005] (see the auxiliary material). In the model it was assumed that settled OC has 28 pMC, while two different scenarios were used for the pMC of CO_2 used for methanogenesis via CO_2 reduction: pure geogenic CO_2 with 0 pMC, and a mixture of 15% (P_{CO2_sed}/IL_{DIC}) biogenic CO_2 derived from the settled OC with pMC 28 and 85% geogenic CO_2 with pMC 0. Simulations were performed for constant steady state CH_4 formation and for the increasing formation rate postulated by *Schmid et al.* [2005]. This analysis consistently showed different contributions of the CH_4 formation pathways below and above the major chemocline. Below the chemocline a large fraction of CH_4 ($f_{CO2} = 65 \pm 5\%$) is produced with old carbon probably originating from geogenic CO_2. Above the chemocline, CH_4 formation from recently settled OC with a maximum of 33% CO_2 reduction [*Conrad*, 1999] can explain the observed radiocarbon ages. The model also reproduced the finer structure of the vertical $^{14}C_{CH4}$ profile (Figure 3b and Figure S1 in Text S1), indicating that it correctly represents the interplay between CH_4 formation from the sediment and the residence times due to the vertical transport in the lake.

[34] An independent estimate of the partitioning between the two pathways below the chemocline was made from the available $\delta^{13}C$ data. In this zone, CH_4 oxidation processes are absent (see sections 4.3.6 and 4.4 for detail). Following the calculations described by *Itoh et al.* [2008], the fraction of CH_4 produced by acetoclastic methanogenesis (F_{Ac}) is calculated by

$$F_{Ac} = \frac{\delta^{13}C_{CH4} - \delta^{13}C_{CH4(CO_2)}}{\delta^{13}C_{CH4(Ac)} - \delta^{13}C_{CH4(CO_2)}}. \quad (3)$$

The isotope ratio of CH_4 from CO_2 reduction ($\delta^{13}C_{CH4(CO2)}$) is estimated by equation (4) from the average of measured $\delta^{13}C_{CO2}$ (−4.9‰, Figure 3d) and using reported ranges of fractionation coefficients for CO_2 reduction from natural bogs and lakes (α_{mc} = 1.06 to 1.073 [*Conrad*, 2005]):

$$\delta^{13}C_{CH4(CO_2)} = \frac{(\delta^{13}C_{CO2} + 1000) - (\alpha_{mc} \cdot 1000)}{\alpha_{mc}} = -61 \text{ to } -70‰. \quad (4)$$

Acetoclastic methanogenesis from organic matter comprises two steps potentially contributing to fractionation: fractionation during the formation of acetate, and fractionation during the actual acetoclastic methanogenesis. We assume that acetate is produced by fermentation and that fractionation between OC and acetate-methyl is negligible (α_{ao} = 1.0 [*Conrad*, 2005]); therefore,

$$\delta^{13}C_{Ac-methyl} = \delta^{13}C_{OC\_sed} = -24‰.$$

The isotope ratio of acetoclastic CH_4 ($\delta^{13}C_{CH4(Ac)}$) can then be estimated using reported ranges of fractionation coefficients for acetoclastic methanogenesis (α_{ma} = 1.007 to 1.027 [*Conrad*, 2005]) analogous to equation (4):

$$\delta^{13}C_{CH4(Ac)} = -31 \text{to } -50‰.$$

Inserting these values into equation (3), we obtain percent contributions of CH_4 formation from CO_2 reduction in the deep water below the chemocline ranging from 43 to 94%, which supports the results of the calculation based on the ^{14}C profile ($f_{CO2} = 65 \pm 5\%$).

[35] However, homoacetogenic formation of acetate from CO_2 could provide a source of acetate with a $\delta^{13}C$ that strongly deviates from $\delta^{13}C_{OC\_sed}$. Although this has mainly been observed under conditions of high acetate accumulation [*Heuer et al.*, 2010], such observations challenge the assumption of $\delta^{13}C_{Ac\text{-}methyl} = \delta^{13}C_{OC\_sed}$. *Conrad et al.* [2010], in a study on tropical lake sediments, found

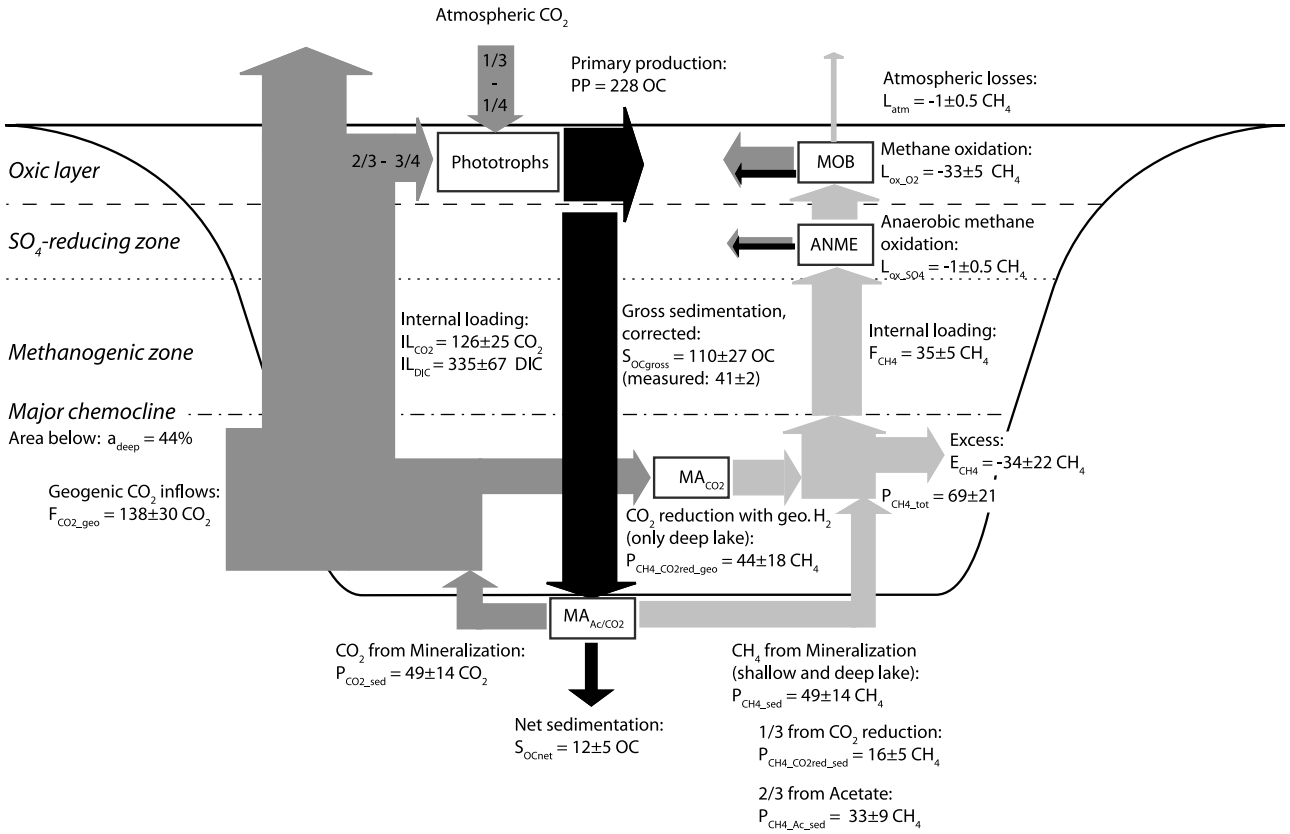

Figure 5. Overview of carbon cycling in Lake Kivu (for details, see section 4.3). CH_4 (light gray), CO_2 (dark gray), and OC (black) fluxes in g C m^{-2} yr^{-1} in Lake Kivu. The dashed line represents the oxycline, the dotted line is the lower boundary of the SO_4^{2-}-reducing zone and the dot-dashed line represents the major chemocline (255 to 262 m depth). All values are areal fluxes and thus do not always add up, as some of them relate to areas smaller than the lake surface. The abbreviations of the fluxes are explained in the text. Boxes indicate microbial populations involved in the process: MA_{Ac}, acetoclastic methanogenic archaea; MA_{CO2}, CO_2-reducing methanogenic archaea; ANME, anaerobic methane oxidizing archaea; MOB, methane oxidizing bacteria (aerobic).

only a nonsignificant correlation between $\delta^{13}C_{Ac\text{-}methyl}$ and $\delta^{13}C_{OC\_sed}$, and observed $\delta^{13}C_{Ac\text{-}methyl}$ to be between 4 and 44‰ more negative than $\delta^{13}C_{OC\_sed}$. While a slightly more negative $\delta^{13}C_{Ac\text{-}methyl}$ would not substantially affect the above estimate, strongly negative values would make it impossible to distinguish acetoclastic methanogenesis from CO_2 reduction by the isotope signature of CH_4. In general, acetogenesis seems to be favored over methanogenesis primarily at low temperatures and high H_2 concentrations [*Heuer et al.*, 2010]. Deep water temperatures in Lake Kivu are 25°C to 26°C [*Schmid et al.*, 2005]. The hydrogen (H_2) concentrations occurring in the sediments are unknown. Acetate in the sediments has not been measured, but in the water column acetate was below detection. Therefore we have no indication that high rates of acetogenesis occur in Lake Kivu. In any case, the net fractionation resulting from homoacetogenesis (using the fractionation factor of 1.06 reported by *Gelwicks et al.* [1989]) and subsequent acetoclastic methanogenesis, is very similar to that resulting from direct reduction of CO_2 by H_2. The occurrence of significant homoacetogenesis would therefore not challenge our conclusions about the fraction of CH_4 derived from CO_2 but only about the pathways for the conversion of CO_2 to CH_4.

[36] Generally, for CH_4 produced only from the degradation of organic matter in the sediment no more than 33% can derive from CO_2 reduction, due to limited amount of H_2 that can form during anaerobic OC degradation [*Conrad*, 1999]:

$$P_{CH4\_CO2red\_sed} = \frac{1}{3} P_{CH4\_sed} = 16 \pm 5 \text{ g C m}^{-2} \text{ yr}^{-1}$$

$$P_{CH4\_Ac\_sed} = \frac{2}{3} P_{CH4\_sed} = 33 \pm 9 \text{ g C m}^{-2} \text{ yr}^{-1}.$$

Below the main chemocline, we assume that 35 ± 5% of CH_4 ($f_{Ac} = 1 - f_{CO2} = 0.35 \pm 0.05$) is derived from acetoclastic methanogenesis and the remainder from CO_2 reduction. The total flux of CH_4 into the compartment below the chemocline is then

$$P_{CH4\_deep} = P_{CH4\_Ac\_sed}/f_{Ac} = 93 \pm 30 \text{ g C m}^{-2} \text{ yr}^{-1}.$$

And the total CH_4 formation from CO_2 reduction is

$$P_{CH4\_CO2red\_deep} = P_{CH4\_Ac\_sed}(1/f_{Ac} - 1) = 61 \pm 22 \text{ g C m}^{-2} \text{ yr}^{-1}.$$

Table 2. Experimental Evidence for Methane Oxidation Determined by Monitoring of Five Bottles per Depth, Kept at in Situ Conditions, 13–20 May 2007, Gisenyi

	Depth				
	20 m	40 m	60 m	80 m	100 m
Methane[a] (μM)					
13.05.2007	0.9	3.6	54	722	1528
14.05.2007	1.3	1.8	53	767	1516
15.05.2007	1.0	1.8	53	727	1571
16.05.2007	1.4	0.9	50	659	1587
17.05.2007	1.2	1.0	50	721	1528
$\delta^{13}C_{CH4}$[b]					
13.05.2007	−59.4	−54.0	−57.2	−54.7	−58.7
17.05.2007	−57.8	−32.0	−57.8		
Apparent methane oxidation rate (nM d^{-1})	ns	618 ± 173	1096 ± 287	ns	ns

[a]Error of measurement is ±1%.
[b]Error of measurement is ±2‰; ns, not significant ($p > 0.05$).

The difference between $P_{CH4\_CO2red\_deep}$ and $P_{CH4\_CO2red\_sed}$ must be produced by an additional pathway that uses old carbon. Here we assume that this pathway is CO_2 reduction with a geogenic H_2 source ($P_{CH4\_CO2red\_geo}$), although geogenic CH_4 is an alternative possibility:

$$P_{CH4\_CO2red\_geo} = P_{CH4\_CO2red\_deep} - P_{CH4\_CO2red\_sed} = \left[\frac{2}{3}(1/f_{Ac} - 1) - \frac{1}{3}\right] P_{CH4\_sed} = 44 \pm 18 \text{ g C m}^{-2} \text{ yr}^{-1}.$$

For steady state, the flux of geogenic CO_2 into the lake water column can now be estimated from internal loading, subtracting CO_2 from mineralization of OC in the sediment (P_{CO2_sed}), and adding the amount of CO_2 reduced by methanogenesis (P_{CH4_CO2red}):

$$F_{CO2\_geo} = IL_{CO2} - P_{CO2\_sed} + P_{CH4\_CO2red\_deep} = 138 \pm 30 \text{ g C m}^{-2} \text{ yr}^{-1}.$$

This parameter might be underestimated given that the lake is probably not at steady state and primary production probably increased since the 1960s [*Pasche et al.*, 2010].

4.3.5. Total Vertical Methane Fluxes

[37] For the sediment area located above the major chemocline we assume, according to our ^{14}C based model, that degradation of organic material (P_{CH4_sed}) is the only CH_4

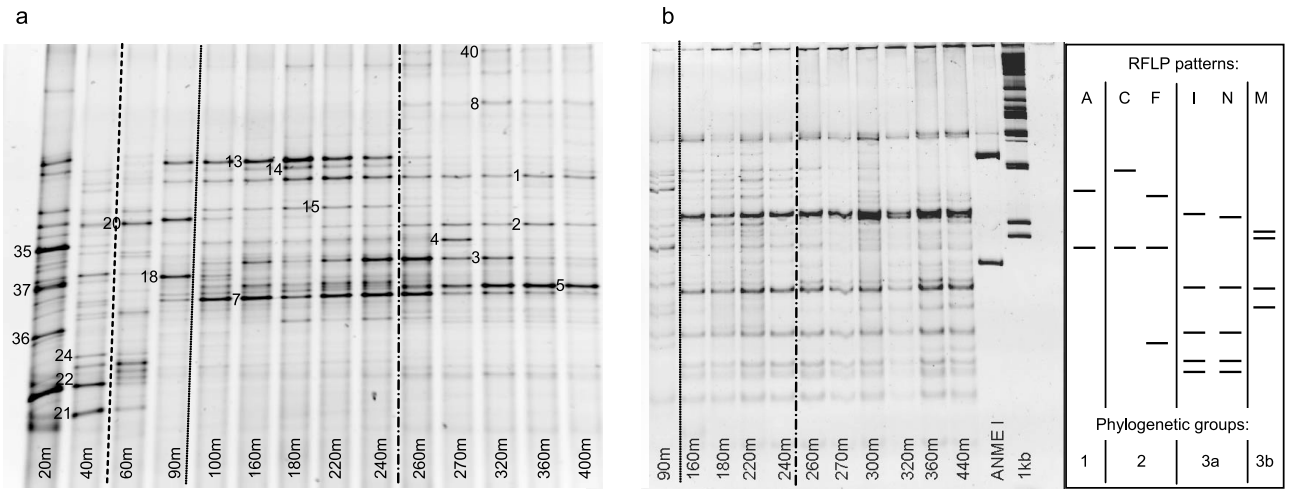

Figure 6. (a) DGGE gel photograph of PCR products obtained with universal bacterial primers 341f-GC and 534r. Samples were taken at 14 depths: in the oxic zone (20 and 40 m depth; dashed line), in the SO_4^{2-}-reducing zone (60 and 90 m; dotted line) and in the anoxic zone (>50 m) that is characterized by increased salinity (up to 6 g L^{-1}) below 260 m (dot-dashed line). Bands which were cut for sequencing are marked to the left of the band. (b) RFLP analyses of *mcrA* gene fragments amplified from the hypolimnion. The pattern of an ANME 1 clone is included as a reference. The patterns of selected RFLP fragment types found in clone libraries (capital letters) are presented to the right. The dotted and dot-dashed lines represent the lower boundary of the SO_4^{2-}-reducing zone and the major chemocline, respectively. No PCR product was obtained for samples above 90 m depth.

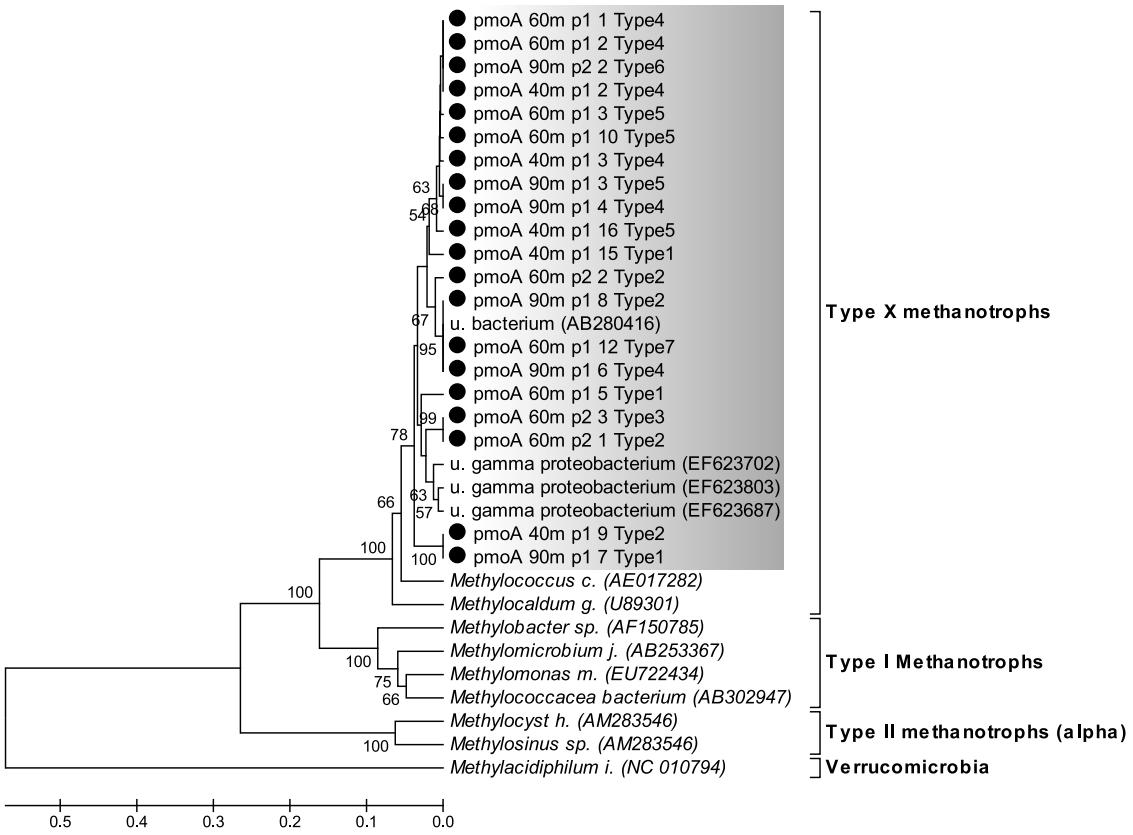

Figure 7. Phylogenetic relationships of PmoA sequences from 0 to 90 m depth (circles) and reference sequences using the UPGMA hierarchical clustering method [*Nei and Kumar*, 2000] and the PAM distance matrix [*Schwarz and Dayhoff*, 1979] as implemented in Mega 4.1, with pairwise gap elimination and 1000 bootstrap resamplings for tree testing. Clone sequences had a length of 166 amino acid residues. The cloned sequences formed two main groups without cultured representatives, which appeared most closely related to PmoA of type X gammaproteobacterial CH_4 oxidizers. Name indicates sample depth, plate number, clone number, and clone phylotype. Scale is number of amino acid substitutions per site.

source. Therefore, the total CH_4 formation averaged over the lake area is

$$P_{CH4\_tot} = a_{shallow}\ P_{CH4\_sed} + a_{deep}\ P_{CH4\_deep} = 69 \pm 21\ \text{g C m}^{-2}\ \text{yr}^{-1},$$

where $a_{shallow} = 0.56$ and $a_{deep} = 0.44$ are the sediment area fractions located at depths <260 m and >260 m, respectively [*Lahmeyer International*, 1998].

[38] CH_4 internal loading, i.e., the total upward flux of CH_4 in the anoxic water column, was independently determined from flux analysis [*Pasche et al.*, 2009]:

$$F_{CH4} = 35 \pm 5\ \text{g C m}^{-2}\ \text{yr}^{-1}.$$

4.3.6. Methane Sinks

[39] Based on model calculation and CH_4 surface concentrations, the loss of CH_4 to the atmosphere was estimated to approximately 1 g C m^{-2} yr^{-1}. A recent thorough analysis by *Borges et al.* [2011] found the loss to the atmosphere to be 0.16 g C m^{-2} yr^{-1}, indicating that we slightly overestimated this flux:

$$L_{atm} = 1 \pm 0.5\ \text{g C m}^{-2}\ \text{yr}^{-1}.$$

The difference between internal loading and loss to the atmosphere comprises the sum of aerobic and anaerobic CH_4 oxidation. The maximum anaerobic CH_4 oxidation with SO_4^{2-} can be calculated from the SO_4^{2-} flux [*Pasche et al.*, 2009]:

$$L_{ox\_SO4} = 1 \pm 0.5\ \text{g C m}^{-2}\ \text{yr}^{-1}.$$

Most of the CH_4 is therefore oxidized aerobically:

$$L_{ox\_O2} = F_{CH4} - L_{atm} - L_{ox\_SO4} = 33 \pm 5\ \text{g C m}^{-2}\ \text{yr}^{-1}.$$

The excess of CH_4 formation, which is currently accumulating in the lake, can be estimated as the difference between CH_4 formation and upward flux:

$$E_{CH4} = P_{CH4\_tot} - F_{CH4} = 34 \pm 22\ \text{g C m}^{-2}\ \text{yr}^{-1}.$$

4.4. Methane Oxidation Incubation Experiment

[40] CH_4 oxidation was verified experimentally with incubation experiments. Significant ($p < 0.05$) decrease of CH_4 over time was only determined at depths 40 and 60 m (Table 2). At 40 m depth, a large proportion of the CH_4 was oxidized during incubation, resulting in a shift of $\delta^{13}C_{CH4}$

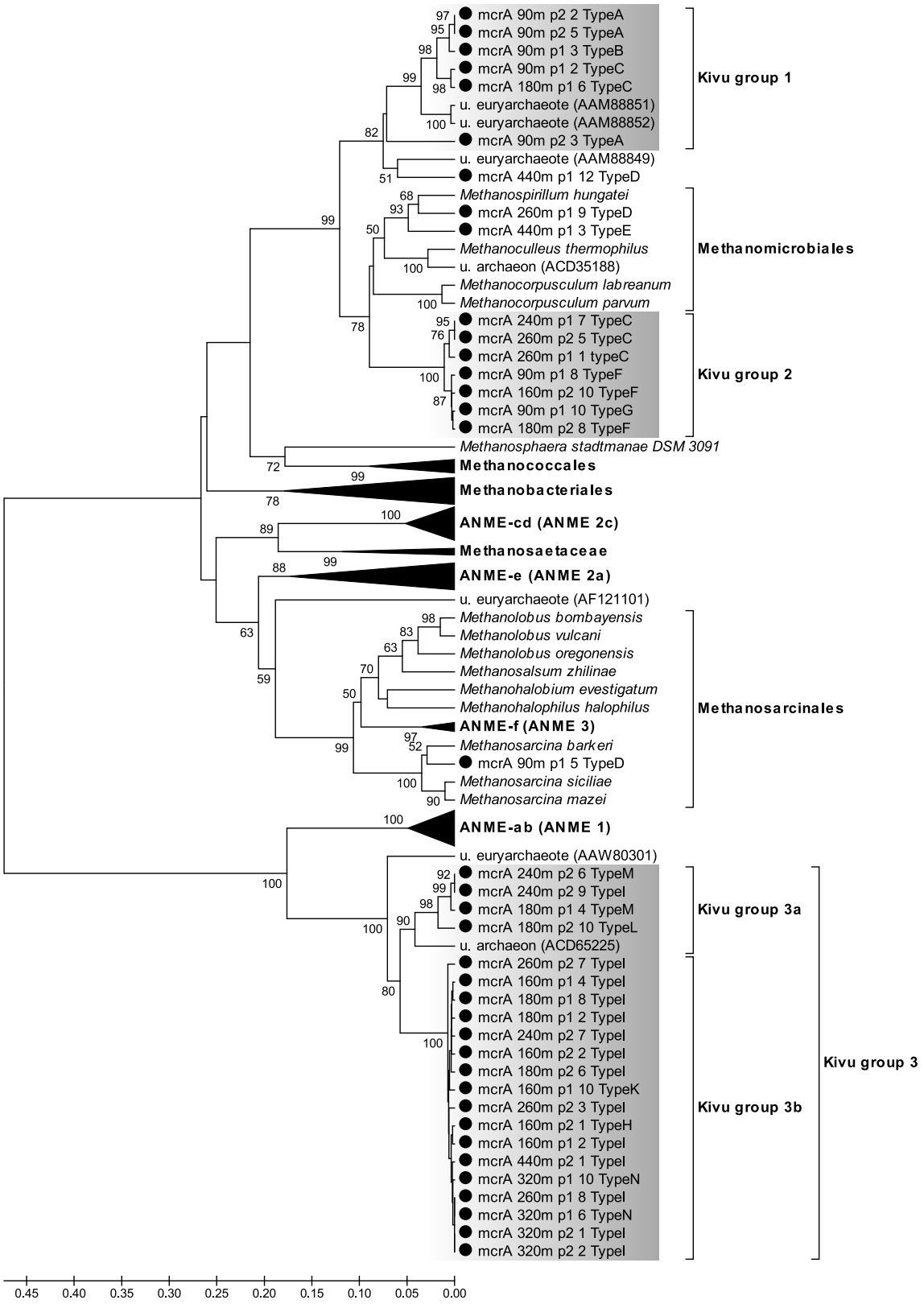

Figure 8. Phylogenetic relationships of McrA sequences from 90 to 440 m depth (circles) and reference sequences using the UPGMA hierarchical clustering method [*Nei and Kumar*, 2000] and the PAM distance matrix [*Schwarz and Dayhoff*, 1979] as implemented in Mega 4.1, with pairwise gap elimination and 1000 bootstrap resamplings for tree testing. Clone sequences had a length of 252 amino acid residues. Kivu groups 1 and 2 appeared closely related to the *Methanomicrobiales*. Group 3 was related to ANME group ab. Scale is number of amino acid substitutions per site.

from −54 to −32‰. A small increase of $\delta^{13}C_{CH4}$ was also observed at 20 m, but was within the error of measurement (±2‰). At 60 m depth, oxygen was depleted at the time of sampling, thus the measured decrease in CH concentration is likely due to anaerobic CH_4 oxidation. Based on published fractionation factors [*Holler et al.*, 2009], a corresponding shift of +1 to +3‰ to a less negative $\delta^{13}C_{CH4}$ would have been expected, which is, however, close to the measurement error, and was not observed. In addition, anaerobic CH_4 oxidation is a process for which low apparent fractionation factors have been reported for environmental samples [*Holler et al.*, 2009]. In summary, results demonstrate active CH_4 oxidation in the 40 m sample, and possibly anaerobic oxidation of CH_4 at 60 m depth. Due to relatively large variations of initial CH_4 concentrations resulting from CH_4 outgassing during filling of the bottles, especially for deep water samples, low rates of CH_4 oxidation would have been undetectable at greater depths.

4.5. Characterization of Microbial Communities

4.5.1. General Microbial Characterization

[41] The bacterial community was characterized using DGGE analysis from amplified 16S rRNA gene fragments (Figure 6a). The community in the oxic (20 and 40 m depth) and in the SO_4^{2-}-reducing (60 and 90 m depth) zones differed strongly from each other and from the deep water community. Between 100 and 260 m depth the community changed little. However, some bands disappeared and some new bands appeared and there were gradual changes in relative band intensity with depth, indicating a slow succession of microbial species in this zone. Below the main chemocline, the community again changed considerably and the number of bands decreased with depth.

[42] Sequencing of excised intense bands (Table S1 in Text S1) revealed typical freshwater bacterial clades in the 20 and 40 m depth samples, e.g., *Actinobacteria* sequences (bands 22, 35, 36). In the hypolimnion several phylotypes closely matched environmental clones from Lake Tanganyika (bands 1, 14, 20), indicating that these are typical components of stratified lakes in the region. An intense band in the SO_4^{2-}-reducing zone (90 m depth, band 18) yielded a *δ-Proteobacterial* sequence with high similarity to SO_4^{2-}-reducing *Desulfocapsa*. Band 4, occurring from 90 to 270 m depth was related to *Lactococcus*, and band 2, occurring from 160 to 400 m depth was classified as belonging to the *Clostridia*, demonstrating the presence of fermenting bacteria among the dominant phylotypes in the hypolimnion.

4.5.2. Aerobic and Anaerobic Methanotrophs

[43] The *pmoA* gene, a marker for aerobic methanotrophs, was readily amplified only from the 40 and 60 m depth samples and weakly from the 90 m sample. Screening and phylogenetic analysis of the clone library created from these amplicons revealed a considerable microdiversity, but all sequenced clones were most closely related to *Methylococcus* and likely represent type X gammaproteobacterial CH_4 oxidizers (Figure 7).

[44] The *mcrA* gene, indicative for methanogenic or anaerobic methanotrophic archaea, was absent from surface waters, but could be PCR-amplified in samples from 90 m depth and below (data not shown). However, RFLP analysis revealed that the 90 m sample (within the SO_4^{2-}-reducing zone) had a community distinct from deeper samples (Figure 6b). Screening of the *mcrA* clone libraries revealed 14 distinct RFLP patterns, and most sequenced clones belonged to three clusters (Kivu groups 1, 2 and 3, Figure 8). Kivu group 1 dominated the 90 m sample library (7 out of 11 clones, 64%) and the most frequent clone RFLP, type (A), is evident as intense bands in the 90 m community RFLP pattern (Figure 6b). Only one representative of this group was found in a library from a greater depth (180 m). Kivu group 2 (Figure 8) was found in libraries from depths 90, 180, 240 and 260 m (1 to 2 clones or ≤20% per library) and its frequent clone types C and F were readily apparent in the community fingerprint (Figure 6b). Both Kivu groups 1 and 2 were most closely related to the *Methanomicrobiales*. Kivu group 3 (with subgroups a and b) was most closely related to the *mcrA* sequences of the ANME-ab clade (associated with ANME 1 [*Hallam et al.*, 2003]) and clearly dominated all clone libraries (60 to 100%) and the community RFLP patterns (Type I and N) in all samples below 90 m depth. The clone RFLP type M was associated with subgroup 3b and appeared to become more abundant below the chemocline according to the community fingerprints. In the 90 m sample, we found no sequences related to group 3, and the clone RFLP patterns associated with this group were not evident in the community fingerprint.

5. Discussion

5.1. Spatial and Temporal Homogeneity of Lake Kivu

[45] By combining data obtained from different sites over a period of five years, we are making assumptions regarding the spatial and temporal homogeneity of Lake Kivu. The chemical and physical data taken over several years and at different locations show that the permanently stratified water column (>60 m depth) is completely homogenous in the horizontal dimension [*Pasche et al.*, 2009]. Chlorophyll and thus primary production is also uniform across the lake, although slightly higher chlorophyll concentrations were found close to the shore [*Kneubühler et al.*, 2007]. This behavior is to be expected, as most of the nutrients stem from the deep water [*Pasche et al.*, 2009], which eliminates any horizontal gradients over the several 100 years of residence. Consistently, sediment cores taken in different parts of the lake reflected the same global changes in lake chemistry [*Pasche et al.*, 2010]. Sedimentation rates and organic matter fluxes however were more variable, e.g., sedimentation rate and TOC flux were 55% and 130% higher in the Gisenyi core compared to the Ishungu core, respectively [*Pasche et al.*, 2010].

[46] Temporal changes in the deep water are notable in the lake, but are slow. The increase in methane concentrations by up to 15% within 30 years [*Schmid et al.*, 2005] corresponds to a change of <0.5% yr^{-1}. All measurements performed within this study were made within a time frame of less than five years. There is no reason to expect changes of more than 2% in the chemical or physical properties of the deep water within this time frame. The only exception from this statement are measurements that are directly related to processes in the surface waters, such as the measured gross sedimentation, which we have corrected for the long-term mean based on available primary productivity data.

5.2. Methanogenesis

5.2.1. Carbon Sources for Methanogenesis

[47] CH_4 in Lake Kivu could be produced by acetoclastic methanogenesis, using acetate produced from OC, or from CO_2 reduction using either geogenic or OC-derived CO_2. Throughout the anoxic water column the CO_2 produced by organic matter fermentation (P_{CO2_sed}, 49 ± 14 g C m^{-2} yr^{-1}) is small compared to the total upward flux of DIC (335 ± 67 g C m^{-2} yr^{-1}) or CO_2 (126 ± 25 g C m^{-2} yr^{-1}) [*Pasche et al.*, 2009]. Geogenic CO_2 (F_{CO2_geo} = 138 ± 30 g C m^{-2} yr^{-1}) is thus far more abundant than CO_2 from mineralization of OC and will be the main substrate for CO_2 reduction. Furthermore, the OC flux observed in sediment traps did not decrease with depth, indicating that mineralization in the anoxic water column is minor [*Pasche et al.*, 2010]. We therefore conclude that acetoclastic methanogenesis in the anoxic water column is limited, although analysis of the *mcrA* gene indicated the presence of a methanogenic population in the water column.

5.2.2. Partitioning Between Methanogenic Pathways

[48] The old age of geogenic CO_2 results in a dead ^{14}C signal (0 pMC). Since Lake Kivu is heavily influenced by geogenic CO_2 this dead radiocarbon strongly influences the apparent ^{14}C ages. This signature can be used to trace the impact of geogenic CO_2 in the system. We observed ^{14}C signals of 28 (15 to 37 cm), 34 (0 to 0.5 cm) and 43 (0.5 to 5 cm) pMC in the sediment OC, while previous measurements resulted in 27 pMC [*Tietze et al.*, 1980]. The observed variability in $^{14}C_{OC}$ cannot be completely explained by the bomb peak [*Manning and Melhuish*, 1994] and might reflect variation in the relative contribution of atmospheric and internally recycled CO_2 to the carbon uptake by primary producers. Modeling of the $^{14}C_{CH4}$ vertical profile in the water column (see section 4.3.4 and Text S1) showed that below 260 m, a large fraction of CH_4 (65 ± 5%) is produced from old carbon. The ^{14}C increase above 260 m results from a combination of the shorter residence time, and a higher proportion (>60%) of CH_4 produced from recently settled OC. The independent estimates of the fraction of CH_4 produced from CO_2 (43 to 94%) based on $\delta^{13}C$ data for CO_2, CH_4, and sediment OC confirmed that this is a realistic estimate. We conclude that below 260 m depth a large fraction (~65%) of CH_4 is produced by reduction of CO_2 with a dead ^{14}C signal, while above 260 m CH_4 is mainly produced from comparatively young OC originating from primary production in the surface mixed layer.

[49] The constant $\delta^{13}C_{CH4}$ and the absence of electron acceptors that could be used for CH_4 oxidation below 100 m, indicated that *mcrA* sequences found in these depths must originate from methanogens, despite the phylogenetic similarity of group Kivu 3 to ANME-ab sequences. The methanogenic archaea in the sediment were not studied, but the presence of unusual *mcrA* groups in the methanogenic zone of the water column indicates that Lake Kivu may harbor an unusual methanogenic community deserving further study.

5.2.3. Origin of Hydrogen

[50] Previous studies have postulated that H_2 used for CO_2 reduction originates from the decomposition of organic matter [*Schoell*, 1980], or from free geogenic H_2 [*Conrad*, 1999; *Deuser et al.*, 1973]. In Lake Kivu we found that below 260 m, only approximately 35% of CH_4 derive from acetoclastic methanogenesis. The δ^2H_{CH4} values of −220‰ in the bottom water are in the range that is typical for carbonate reduction (−250 to −150‰) [*Whiticar*, 1999], supporting the notion that CO_2 reduction is a dominant process in the deep water. A considerable amount of H_2 is required to account for the formation of the remaining 65% ($P_{CH4\_CO2red\_geo}$ = 44 ± 18 g C m^{-2} yr^{-1}) of CH_4 through CO_2 reduction. An additional source of H_2 is therefore necessary to explain our findings.

[51] At the moment we can only speculate on the source of this additional H_2. The gases from Nyiragongo volcano north of Lake Kivu contained only low amounts of H_2 (<2 vol %), also relative to CO_2 (≤1% of CO_2 [*Gerlach*, 1980; *Le Guern*, 1987; *Tedesco et al.*, 2007]). Applying this ratio to the geogenic CO_2 influx (138 ± 30 g C m^{-2} yr^{-1}), this H_2 could only account for <1.4 g C_{CH4} m^{-2} yr^{-1}. Considerably higher H_2 concentrations (23% of CO_2) have been observed in gas bubbles collected in the lake near the lava front of the 2002 Nyiragongo eruption. The source of these gases remains unclear [*Tedesco et al.*, 2007], but nevertheless this may indicate that inflows of groundwater that has been in contact with juvenile gases could be a significant source of H_2. H_2 could also be formed by chemical processes, e.g., pyrite precipitation [*Rickard*, 1997]. An alternative explanation for our observations would be a direct inflow of geogenic CH_4, formed during the cooling of magmatic gases at depth in the absence of oxygen [*Gerlach*, 1980], which would likewise have a dead ^{14}C signal and high δ^2H_{CH4} [*Whiticar*, 1999].

5.2.4. Methane Fluxes

[52] The CH_4 release estimated from the Gisenyi sediment core ranged between 60 and 100 g C_{CH4} m^{-2} yr^{-1} (Figure 5). The upper flux estimate is too high to be explained by the available sedimenting OC but the lower estimate falls within the range calculated from OC gross and net sedimentation (P_{CH4_sed} = 49 ± 14 g C_{CH4} m^{-2} yr^{-1}) after correcting for the unusually low primary productivity during the two years of our sediment trap deployment [*Pasche et al.*, 2010]. Based on the considerations in sections 4.3.4 and 5.2.2, we propose that this flux represents the total CH_4 formation above 260 m but only ~53% of the CH_4 formation below 260 m. Below 260 m, the additional geogenic CH_4 leads to a total formation of 93 ± 30 g C_{CH4} m^{-2} yr^{-1} (P_{CH4_deep}).

5.2.5. Methane Budget and Accumulation

[53] CH_4 concentrations seem to have increased by up to 15% based on measurements made in 1975 and 2004. Our estimate of CH_4 accumulation (E_{CH4} = 34 ± 22 g C_{CH4} m^{-2} yr^{-1}) is still imprecise, but strongly indicates that CH_4 currently accumulates in the lake. Several observations further support the hypothesis of a recent increase in CH_4 concentrations in Lake Kivu. The ^{14}C signal in dissolved CH_4 (11.4 pMC) has increased since 1975 (9 pMC [*Tietze*, 1978]). In the same time span, $\delta^{13}C_{CH4}$ decreased from −57‰ [*Tietze et al.*, 1980] to −59.8‰. These differences in the CH_4 isotopic values are not significant, as they are within the uncertainty range of a comparison of the historic and recent measurements, but they are both consistent with an increased formation of CH_4 with isotopic signatures observed in the surface sediment (34 pMC, $\delta^{13}C$ = −65‰). Furthermore, OC mass accumulation in the sediment has increased by 20% since the 1960s, when carbonates suddenly started to precipitate [*Pasche et al.*, 2010]. However, the calculated range of E_{CH4} (34 ± 22 g C_{CH4} m^{-2} yr^{-1}) does not allow for the

excess required (~75 g C_{CH4} m^{-2} yr^{-1}) to explain the observed CH_4 increase over the last decades [*Schmid et al.*, 2005]. In summary, the analysis supports the hypothesis that CH_4 concentrations in Lake Kivu are currently increasing, but probably at a lower rate than previously assumed.

[54] We propose that several concurrent environmental changes might have increased OC sedimentation [*Pasche et al.*, 2010]. First, an increase of the subaquatic inflows [*Schmid et al.*, 2010], potentially caused by higher rainfall observed during 1961 to 1990 in eastern Africa [*Nicholson and Yin*, 2001], might have led to stronger uplift and consequently greater supply of nutrients. Second, recent external P and N inputs might have increased due to the fast growing population [*Muvundja et al.*, 2009]. Third, the introduction of *Limnothrissa miodon* strongly altered the food web, which might have modified the exported OC [*Isumbisho et al.*, 2006]. As a large proportion of CH_4 seems to be produced from geogenic H_2, we cannot exclude that geogenic inputs have also increased, especially in this geologically active region.

5.3. Methane Oxidation

[55] CH_4 oxidation was confirmed by incubation experiments, the heavier $^{13}C_{CH4}$ in the water layers above 90 m depth, and the presence of specific microbial communities. The determined rates (618 ± 173 and 1096 ± 287 nM d^{-1}) were an order of magnitude higher than those observed in marine environments with relatively high CH_4 concentrations [*Kelley*, 2003] (up to 57 nM d^{-1}) but in the same range as reported for Lake Tanganyika [*Rudd*, 1980] (up to 1920 nM d^{-1}). Comparing $^{13}C_{CH4}$ to electron acceptor depth profiles indicates two major zones for CH_4 oxidation: the oxic layer (0 to 50 m); and the SO_4^{2-}-reducing zone (60 to 90 m). Concentrations of other potential electron acceptors for anaerobic CH_4 oxidation, i.e., nitrate [*Ettwig et al.*, 2010] and oxidized iron and manganese ions [*Beal et al.*, 2009] were too low to significantly oxidize CH_4. At 90 m depth, near the lower end of the SO_4^{2-}-reducing zone, we detected a dominant distinct clade of *mcrA* genes with closest matches to the *Methanomicrobiales*, which could potentially represent a new ANME group. A potential SO_4^{2-}-reducing partner related to *Desulfocapsa* was identified from the general bacterial DGGE (band 18). Flux analyses [*Pasche et al.*, 2009] showed that the SO_4^{2-} flux can oxidize a maximum of 3% (1 ± 0.5 g C m^{-2} yr^{-1}) of the CH_4 upward flux (35 ± 5 g C m^{-2} yr^{-1}). The 3% is probably overestimated, as sulfate reducers can also use organic matter or H_2 as electron donors. In conclusion, anaerobic CH_4 oxidation takes place in Lake Kivu and may involve unique microbial populations but represents only a minor CH_4 sink. This is in contrast to neighboring Lake Tanganyika, where anaerobic CH_4 oxidation consumes about half of the CH_4 transported upwards from the deep waters [*Durisch-Kaiser et al.*, 2011]. The reason for the higher importance of anaerobic CH_4 oxidation is the much higher relative occurrence of SO_4^{2-} to CH_4 in Lake Tanganyika (maximum concentrations 40 μM SO_4^{2-} to 150 μM CH_4) compared to Lake Kivu (150 μM SO_4^{2-} to 20,000 μM CH_4).

[56] Conversely, aerobic CH_4 oxidation is the main sink for CH_4 in Lake Kivu. In addition to the experimental verification of CH_4 oxidation at 40 and 60 m depth we also observed that the $^{13}C_{CH4}$ isotopic signal showed marked (10‰) enrichment at the oxycline (Figure 3). The *pmoA* gene, a marker for aerobic methanotrophs, was also detected in the oxycline in the 40 and 60 m depth samples. The cloned sequences were most closely related to *Methylococcus capsulatus* (type X). However, a more diverse community of CH_4 oxidizers could be present, as the used primer set was reported to have a potential bias toward type X methanotrophs [*McDonald et al.*, 2008; *Rahalkar and Schink*, 2007]. Flux analyses revealed that the O_2 flux (oxidation potential 57 g C m^{-2} yr^{-1}) was higher than the CH_4 upward flux (35 ± 5 g C $m^{-2}yr^{-1}$) and has the potential to oxidize most of the CH_4 present, even if O_2 is shared to oxidize other electron donors [*Pasche et al.*, 2009]. We estimate an oxidation rate of 33 ± 5 g C m^{-2} yr^{-1} (section 4.3.6), as the CH_4 release to the atmosphere is low. The oxidation rate agrees well with a previous estimate (31 g C m^{-2} yr^{-1}) for Lake Kivu [*Jannasch*, 1975]. Aerobic CH_4 oxidation has been estimated to 37 g C m^{-2} yr^{-1} for Lake Tanganyika [*Rudd*, 1980], which is, however, not supported by the estimated areal CH_4 formation of 6 g C m^{-2} yr^{-1} [*Durisch-Kaiser et al.*, 2011].

6. Conclusion

[57] Lake Kivu is a unique ecosystem with extremely high CH_4 concentrations. The lake's volcanic setting provides high quantities of geogenic CO_2. In the deep water, about 65% of the CH_4 originates from dead carbon, suggesting the input of geogenic H_2 or CH_4. The flux analysis as well as several changes in the hydrological and ecological dynamics of Lake Kivu qualitatively support the previously observed CH_4 increase [*Schmid et al.*, 2005]. CH_4 is mainly oxidized by type X CH_4-oxidizing bacteria at the oxycline, while anaerobic CH_4 oxidation plays a minor role, but may involve a novel cluster of ANME.

[58] **Acknowledgments.** We are grateful to Michael Schurter, Christian Dinkel, Georges Alunga, and Fabrice Muvundja for water and gas sampling; to Torsten Diem and Oliver Scheidegger for their support on gas and isotopes measurements; to Katrin Knittel for providing ANME *mcrA* reference clones, to Päivi Rinta and Martin Schroth for the measurement of organic anions; and to Eawag's AUA laboratory for determining TOC concentrations. We are especially thankful to Bernhard Wehrli and the anonymous reviewers of previous versions of the manuscript for instructive discussions and comments. The project was supported by the Swiss National Science Foundation, internal Eawag funds, and the Swiss Agency for Development and Cooperation under grant 207021-109710 (Nutrient cycling in Lake Kivu).

References

Altschul, S. F., W. Gish, W. Miller, E. W. Myers, and D. J. Lipman (1990), Basic local alignment search tool, *J. Mol. Biol.*, *215*, 403–410, doi:10.1016/S0022-2836(05)80360-2.

Bastviken, D., J. Cole, M. Pace, and L. Tranvik (2004), Methane emissions from lakes: Dependence of lake characteristics, two regional assessments, and a global estimate, *Global Biogeochem. Cycles*, *18*, GB4009, doi:10.1029/2004GB002238.

Beal, E. J., C. H. House, and V. J. Orphan (2009), Manganese- and iron-dependent marine methane oxidation, *Science*, *325*(5937), 184–187, doi:10.1126/science.1169984.

Bergamino, N., S. Horion, S. Stenuite, Y. Cornet, S. Loiselle, P. D. Plisnier, and J. P. Descy (2010), Spatio-temporal dynamics of phytoplankton and primary production in Lake Tanganyika using a MODIS based bio-optical time series, *Remote Sens. Environ.*, *114*(4), 772–780, doi:10.1016/j.rse.2009.11.013.

Borges, A. V., G. Abril, B. Delille, J.-P. Descy, and F. Darchambeau (2011), Diffusive methane emissions to the atmosphere from Lake Kivu (eastern Africa), *J. Geophys. Res.*, doi:10.1029/2011JG001673, in press.

Bourne, D. G., I. R. McDonald, and J. C. Murrell (2001), Comparison of pmoA PCR primer sets as tools for investigating methanotroph diversity

in three Danish soils, *Appl. Environ. Microbiol.*, *67*(9), 3802–3809, doi:10.1128/AEM.67.9.3802-3809.2001.

Conrad, R. (1999), Contribution of hydrogen to methane production and control of hydrogen concentrations in methanogenic soils and sediments, *FEMS Microbiol. Ecol.*, *28*, 193–202, doi:10.1111/j.1574-6941.1999.tb00575.x.

Conrad, R. (2005), Quantification of methanogenic pathways using stable carbon isotopic signatures: A review and a proposal, *Org. Geochem.*, *36*, 739–752, doi:10.1016/j.orggeochem.2004.09.006.

Conrad, R., M. Noll, P. Claus, M. Klose, W. R. Bastos, and A. Enrich-Prast (2010), Stable carbon isotope discrimination and microbiology of methane formation in tropical anoxic lake sediments, *Biogeosciences Discuss.*, *7*(6), 8619–8661, doi:10.5194/bgd-7-8619-2010.

Deuser, W. G., E. T. Degens, and G. T. Harvey (1973), Methane in Lake Kivu: New data bearing on its origins, *Science*, *181*, 51–54, doi:10.1126/science.181.4094.51.

Durisch-Kaiser, E., M. Schmid, F. Peeters, R. Kipfer, C. Dinkel, T. Diem, C. J. Schubert, and B. Wehrli (2011), What prevents outgassing of methane to the atmosphere in Lake Tanganyika?, *J. Geophys. Res.*, *116*, G02022, doi:10.1029/2010JG001323.

Earl, J., G. Hall, R. W. Pickup, D. A. Ritchie, and C. Edwards (2003), Analysis of methanogen diversity in a hypereutrophic lake using PCR-RFLP analysis of *mcr* sequences, *Microb. Ecol.*, *46*, 270–278, doi:10.1007/s00248-003-2003-x.

Ettwig, K. F., et al. (2010), Nitrite-driven anaerobic methane oxidation by oxygenic bacteria, *Nature*, *464*(7288), 543–548, doi:10.1038/nature08883.

Gelwicks, J. T., J. B. Risatti, and J. M. Hayes (1989), Carbon isotope effects associated with autotrophic acetogenesis, *Org. Geochem.*, *14*(4), 441–446, doi:10.1016/0146-6380(89)90009-0.

Gerlach, T. M. (1980), Chemical characteristics of the volcanic gases from Nyiragongo lava lake and the generation of CH_4-rich fluid inclusions in alkaline rocks, *J. Volcanol. Geotherm. Res.*, *8*, 177–189, doi:10.1016/0377-0273(80)90103-1.

Hajdas, I., S. D. Ivy, J. Beer, G. Bonani, D. Imboden, A. F. Lotter, M. Sturm, and M. Suter (1993), AMS radiocarbon dating and varve chronology of Lake Soppensee: 6000 to 12000 ^{14}C years B P, *Clim. Dyn.*, *9*, 107–116, doi:10.1007/BF00209748.

Hales, B. A., C. Edwards, D. A. Ritchie, G. Hall, R. W. Pickup, and J. R. Saunders (1996), Isolation and identification of methanogen-specific DNA from blanket bog peat by PCR amplification and sequence analysis, *Appl. Environ. Microbiol.*, *62*(2), 668–675.

Hallam, S. J., P. R. Girguis, C. M. Preston, P. M. Richardson, and E. F. DeLong (2003), Identification of methyl coenzyme M reductase A (*mcr*A) genes associated with methane-oxidizing archaea, *Appl. Environ. Microbiol.*, *69*(9), 5483–5491, doi:10.1128/AEM.69.9.5483-5491.2003.

Heuer, V. B., M. Krüger, M. Elvert, and K. U. Hinrichs (2010), Experimental studies on the stable carbon isotope biogeochemistry of acetate in lake sediments, *Org. Geochem.*, *41*(1), 22–30, doi:10.1016/j.orggeochem.2009.07.004.

Hinrichs, K. U., and A. Boetius (2002), The anaerobic oxidation of methane: New insights in microbial ecology and biogeochemistry, in *Ocean Margin Systems*, edited by G. Wefer et al., pp. 457–477, Springer, Berlin.

Holler, T., G. Wegener, K. Knittel, A. Boetius, B. Brunner, M. M. M. Kuypers, and F. Widdel (2009), Substantial ^{13}C/^{12}C and D/H fractionation during anaerobic oxidation of methane by marine consortia enriched in vitro, *Environ. Microbiol. Rep.*, *1*(5), 370–376, doi:10.1111/j.1758-2229.2009.00074.x.

Isumbisho, M., H. Sarmento, B. Kaningini, J.-C. Micha, and J.-P. Descy (2006), Zooplankton of Lake Kivu, East Africa, half a century after the Tanganyika sardine introduction, *J. Plankton Res.*, *28*(11), 971–989, doi:10.1093/plankt/fbl032.

Itoh, M., N. Ohte, K. Koba, A. Sugimoto, and M. Tani (2008), Analysis of methane production pathways in a riparian wetland of a temperate forest catchment, using δ^{13}C of pore water CH_4 and CO_2, *J. Geophys. Res.*, *113*, G03005, doi:10.1029/2007JG000647.

Jannasch, H. W. (1975), Methane oxidation in Lake Kivu (central Africa), *Limnol. Oceanogr.*, *20*(5), 860–864, doi:10.4319/lo.1975.20.5.0860.

Jones, N. (2003), Chock-full of methane, Lake Kivu stores enough energy to power all of Rwanda, *New Sci.*, *2384*, 17.

Kelley, C. (2003), Methane oxidation potential in the water column of two diverse coastal marine sites, *Biogeochemistry*, *65*(1), 105–120, doi:10.1023/A:1026014008478.

Kessler, J. D., and W. S. Reeburgh (2005), Preparation of natural methane samples for stable isotope and radiocarbon analysis, *Limnol. Oceanogr. Methods*, *3*, 408–418.

Kling, G. W., M. A. Clark, H. R. Compton, J. D. Devine, W. C. Evans, A. M. Humphrey, E. J. Koenigsberg, J. P. Lockwood, M. L. Tuttle, and G. N. Wagner (1987), The 1986 Lake Nyos gas disaster in Cameroon, West Africa, *Science*, *236*, 169–175, doi:10.1126/science.236.4798.169.

Kneubühler, M., T. Frank, T. W. Kellenberger, N. Pasche, and M. Schmid (2007), Mapping chlorophyll-a in Lake Kivu with remote sensing methods, in *Proceedings of the ENVISAT Symposium Montreux*, ESA Publ. Div., Nordwijk, Netherlands.

Lahmeyer International (1998), Bathymetric survey of Lake Kivu, final report, 18 pp, Minist. of Public Work, Dir. of Energy and Hydrocarbons, Kigali, Rwanda.

Larkin, M. A., et al. (2007), Clustal W and Clustal X version 2.0, *Bioinformatics*, *23*, 2947–2948, doi:10.1093/bioinformatics/btm404.

Le Guern, F. (1987), Mechanism of energy transfer in the lava lake of Nyiragongo (Zaire), 1959–1977, *J. Volcanol. Geotherm. Res.*, *31*, 17–31, doi:10.1016/0377-0273(87)90003-5.

Llirós, M., E. O. Casamayor, and C. Borrego (2008), High archaeal richness in the water column of a freshwater sulfurous karstic lake along an interannual study, *FEMS Microbiol. Ecol.*, *66*, 331–342, doi:10.1111/j.1574-6941.2008.00583.x.

Manning, M. R., and W. H. Melhuish (Eds.) (1994), *Atmospheric $\delta^{14}C$ Record From Wellington*, Carbon Dioxide Inf. Anal. Cent., Oak Ridge Natl. Lab., U.S. Dep. of Energy, Oak Ridge, Tenn.

McAuliffe, C. (1971), GC determination of solutes by multiple phase equilibration, *Chemtech*, *1*(1), 46–51.

McDonald, I. R., L. Bodrossy, Y. Chen, and J. C. Murrell (2008), Molecular ecology techniques for the study of aerobic methanotrophs, *Appl. Environ. Microbiol.*, *74*(5), 1305–1315, doi:10.1128/AEM.02233-07.

Müller, B., Y. Wang, M. Dittrich, and B. Wehrli (2003), Influence of organic carbon decomposition on calcite dissolution in surficial sediments of a freshwater lake, *Water Res.*, *37*(18), 4524–4532, doi:10.1016/S0043-1354(03)00381-6.

Muvundja, F., N. Pasche, F. W. B. Bugenyi, M. Isumbisho, B. Müller, J. N. Namugize, P. Rinta, M. Schmid, R. Stierli, and A. Wüest (2009), Balancing nutrient inputs to Lake Kivu, *J. Great Lakes Res.*, *35*(3), 406–418, doi:10.1016/j.jglr.2009.06.002.

Muyzer, G., E. C. De Waal, and G. Uitierlinden (1993), Profiling of complex microbial populations by denaturing gradient gel electrophoresis analysis of polymerase chain reaction-amplified genes coding for 16S rRNA, *Appl. Environ. Microbiol.*, *59*(3), 695–700.

Nei, M., and S. Kumar (2000), *Molecular Evolution and Phylogenetics*, 333 pp., Oxford Univ. Press, New York.

Nicholson, S. E., and X. Yin (2001), Rainfall conditions in equatorial East Africa during the nineteenth century as inferred from the record of Lake Victoria, *Clim. Change*, *48*(2/3), 387–398, doi:10.1023/A:1010736008362.

Pasche, N., C. Dinkel, B. Müller, M. Schmid, A. Wüest, and B. Wehrli (2009), Physical and biogeochemical limits to internal nutrient loading of meromictic Lake Kivu, *Limnol. Oceanogr.*, *54*, 1863–1873, doi:10.4319/lo.2009.54.6.1863.

Pasche, N., G. Alunga, K. Mills, F. Muvundja, D. Ryves, M. Schurter, B. Wehrli, and M. Schmid (2010), Abrupt onset of carbonate deposition in Lake Kivu during the 1960s: Response to recent environmental changes, *J. Paleolimnol.*, *44*(4), 931–946, doi:10.1007/s10933-010-9465-x.

Rahalkar, M., and B. Schink (2007), Comparison of aerobic methanotrophic communities in littoral and profundal sediments of Lake Constance by a molecular approach, *Appl. Environ. Microbiol.*, *73*(13), 4389–4394, doi:10.1128/AEM.02602-06.

Rickard, D. (1997), Kinetics of pyrite formation by the H_2S oxidation of iron (II) monosulfide in aqueous solutions between 25 and 125°C: The rate equation, *Geochim. Cosmochim. Acta*, *61*(1), 115–134, doi:10.1016/S0016-7037(96)00321-3.

Rudd, J. W. M. (1980), Methane oxidation in Lake Tanganyika (East Africa), *Limnol. Oceanogr.*, *25*(5), 958–963, doi:10.4319/lo.1980.25.5.0958.

Sansone, F. J., B. N. Popp, and T. M. Rust (1997), Stable carbon isotopic analysis of low-level methane in water and gas, *Anal. Chem.*, *69*(1), 40–44, doi:10.1021/ac960241i.

Sarmento, H., M. Isumbisho, S. Stenuite, F. Darchambeau, B. Leporcq, and J.-P. Descy (2009), Phytoplankton ecology of Lake Kivu (eastern Africa): Biomass, production and elemental ratios, *Verh. Int. Verein. Limnol.*, *30*(5), 709–713.

Schmid, M., K. Tietze, M. Halbwachs, A. Lorke, D. McGinnis, and A. Wüest (2004), How hazardous is the gas accumulation in Lake Kivu? Arguments for a risk assessment in light of the Nyiragongo Volcano eruption of 2002, *Acta Vulcanol.*, *14/15*, 115–121.

Schmid, M., M. Halbwachs, B. Wehrli, and A. Wüest (2005), Weak mixing in Lake Kivu: New insights indicate increasing risk of uncontrolled gas eruption, *Geochem. Geophys. Geosyst.*, *6*, Q07009, doi:10.1029/2004GC000892.

Schmid, M., M. Busbridge, and A. Wüest (2010), Double-diffusive convection in Lake Kivu, *Limnol. Oceanogr.*, *55*(1), 225–238, doi:10.4319/lo.2010.55.1.0225.

Schoell, M. (1980), The hydrogen and carbon isotopic composition of methane from natural gases of various origins, *Geochim. Cosmochim. Acta*, *44*, 649–661, doi:10.1016/0016-7037(80)90155-6.

Schoell, M., K. Tietze, and S. M. Schoberth (1988), Origin of methane in Lake Kivu (east-central Africa), *Chem. Geol.*, *71*, 257–265, doi:10.1016/0009-2541(88)90119-2.

Schubert, C. J., F. S. Lucas, E. Durisch-Kaiser, R. Stierli, T. Diem, O. Scheidegger, F. Vazquez, and B. Müller (2010), Oxidation and emission of methane in a monomictic lake (Rotsee, Switzerland), *Aquat. Sci.*, *72*(4), 455–466, doi:10.1007/s00027-010-0148-5.

Schwarz, R., and M. Dayhoff (1979), Matrices for detecting distant relationships, in *Atlas of Protein Sequences*, edited by M. Dayhoff, pp. 353–358, Natl. Biomed. Res. Found., Washington, D. C.

Sigurdsson, H., J. D. Devine, F. M. Tchoua, T. S. Presser, M. K. W. Pringle, and W. C. Evans (1987), Origin of the lethal gas burst from Lake Monoun, Cameroun, *J. Volcanol. Geotherm. Res.*, *31*, 1–16, doi:10.1016/0377-0273(87)90002-3.

Sobek, S., E. Durisch-Kaiser, R. Zurbrügg, N. Wongfun, M. Wessels, N. Pasche, and B. Wehrli (2009), Organic carbon burial efficiency in lake sediments controlled by oxygen exposure time and sediment source, *Limnol. Oceanogr.*, *54*(6), 2243–2254, doi:10.4319/lo.2009.54.6.2243.

Stuiver, M., and H. A. Polach (1977), Discussion: Reporting ^{14}C data, *Radiocarbon*, *19*, 355–363.

Tamura, K., J. Dudley, M. Nei, and S. Kumar (2007), MEGA4: Molecular Evolutionary Genetics Analysis (MEGA) software version 4.0, *Mol. Biol. Evol.*, *24*, 1596–1599, doi:10.1093/molbev/msm092.

Tedesco, D., O. Vaselli, P. Papale, S. A. Carn, M. Voltaggio, G. M. Sawyer, J. Durieux, M. Kasereka, and F. Tassi (2007), January 2002 volcano-tectonic eruption of Nyiragongo volcano, Democratic Republic of Congo, *J. Geophys. Res.*, *112*, B09202, doi:10.1029/2006JB004762.

Tietze, K. (1978), Geophysikalische Untersuchung des Kivusees und seiner ungewöhnlichen Methangaslagerstätte—Schichtung, Dynamik und Gasgehalt des Seewassers, es Sciences thesis, 150 pp., Christian-Albrechts-Univ., Kiel, Germany.

Tietze, K., M. Geyh, H. Müller, L. Schröder, W. Stahl, and H. Wehner (1980), The genesis of methane in Lake Kivu (central Africa), *Geol. Rundsch.*, *69*, 452–472, doi:10.1007/BF02104549.

Wang, Q., G. M. Garrity, J. M. Tiedje, and J. R. Cole (2007), Naïve Bayesian classifier for rapid assignment of rRNA sequences into the new bacterial taxonomy, *Appl. Environ. Microbiol.*, *73*(16), 5261–5267, doi:10.1128/AEM.00062-07.

Whiticar, M. J. (1999), Carbon and hydrogen isotope systematics of bacterial formation and oxidation of methane, *Chem. Geol.*, *161*, 291–314, doi:10.1016/S0009-2541(99)00092-3.

Wiesenburg, D. A., and N. L. Guinasso (1979), Equilibrium solubilities of methane, carbon-monoxide, and hydrogen in water and sea water, *J. Chem. Eng. Data*, *24*, 356–360, doi:10.1021/je60083a006.

H. Bürgmann, M. Schmid, C. J. Schubert, F. Vazquez, and A. Wüest, Eawag: Swiss Federal Institute of Aquatic Science and Technology, Surface Waters—Research and Management, CH-6047 Kastanienbaum, Switzerland. (Helmut.Buergmann@eawag.ch)

J. D. Kessler, Department of Oceanography, Texas A&M University, College Station, TX 77843-3146, USA.

M. A. Pack and W. S. Reeburgh, Department of Earth System Science, University of California, Irvine, CA 92697-3100, USA.

N. Pasche, Lake Kivu Monitoring Program, Ministry of Infrastructure, Gisenyi, Rwanda.

JOURNAL OF GEOPHYSICAL RESEARCH
Biogeosciences
AN AGU JOURNAL

Free Access

What prevents outgassing of methane to the atmosphere in Lake Tanganyika?

Edith Durisch-Kaiser Martin Schmid Frank Peeters Rolf Kipfer Christian Dinkel Torsten Diem
Carsten J. Schubert Bernhard Wehrli

First published: 16 June 2011 https://doi.org/10.1029/2010JG001323 Citations: 11

Abstract

[1] Tropical East African Lake Tanganyika hosts the Earth's largest anoxic freshwater body. The entire water column holds over 23 Tg of the potent greenhouse gas methane (CH_4). Methane is formed under sulphate-poor conditions via carbon dioxide reduction or fermentation from detritus and relict sediment organic matter. Permanent density stratification supports an accumulation of CH_4 below the permanent oxycline. Despite CH_4 significance for global climate, anaerobic microbial consumption of CH_4 in freshwater is poorly understood. Here we provide evidence for intense methanotrophic activity not only in the oxic but also in the anoxic part of the water column of Lake Tanganyika. We measured CH_4, ^{13}C of dissolved CH_4, dissolved oxygen (O_2), sulphate (SO_4^{2-}), sulphide (HS^-) and the transient tracers chlorofluorocarbon-12 (CFC-12) and tritium (^3H). A basic one-dimensional model, which considers vertical transport and biogeochemical fluxes and transformations, was used to interpret the vertical distribution of these substances. The results suggest that the anaerobic oxidation of CH_4 is an important mechanism limiting CH_4 to the anoxic zone of Lake Tanganyika. The important role of the anaerobic oxidation for CH_4 concentrations is further supported by high abundances (up to ~33% of total DAPI-stained cells) of single living archaea, identified by fluorescence in situ hybridization

1. Introduction

[2] East African tropical lakes store approximately one quarter of the Earth's freshwater [***Bootsma and Hecky*, 2003**]. Although they bear large amounts of the greenhouse gases CO_2 and CH_4 in their water bodies [***Deuser et al.*, 1973**; ***Rudd*, 1980**; ***Schmid et al.*, 2005**], their contribution to the natural source of CH_4 to the atmosphere is to date unknown. Furthermore, there is growing evidence that lakes may represent significant sources of greenhouse gases and may dominate total natural CH_4 emissions [***Bastviken et al.*, 2004**]. However, quantification is

often difficult, due to spatially and temporally variable emission rates [***International Panel on Climate Control*, 2007**; ***Van der Nat and Middelburg*, 2000**] and pathways [***Bastviken et al.*, 2004**].

[3] In the ocean, only little CH_4 ever escapes to the atmosphere. Most CH_4 is scavenged by anaerobic microbial oxidation according to $CH_4 + SO_4^{2-} \rightarrow HCO_3^- + HS^- + H_2O$ [***Valentine and Reeburgh*, 2000**]. Archaeal groups in association with sulphate-reducing bacteria were shown to mediate this process. Most of these marine archaea are related to the Methanosarcinales [***Boetius et al.*, 2000**; ***Michaelis et al.*, 2002**; ***Schubert et al.*, 2006**] and are associated with sulphate-reducing bacteria, widely linked to the *Desulfosarcina*/*Desulfococcus* cluster (Deltaproteobacteria). For lacustrine systems only a small suite of studies exist, which prove the occurrence of anaerobic oxidation of CH_4 [e.g., ***Iversen and Jorgensen*, 1985**; ***Panganiban et al.*, 1979**; ***Smemo and Yavitt*, 2007**]. To date only two mechanisms other than the one coupled to sulphate reduction are known, namely manganese and iron reduction and denitrification [***Beal et al.*, 2009**; ***Raghoebarsing et al.*, 2006**]. These mechanisms were reported from incubations under laboratory conditions or from seep sediment and have not yet been confirmed to occur in lakes. Conditions for anaerobic oxidation of CH_4 are less favorable in freshwater systems, because sulphate and dissolved metal concentrations are generally low and easily become the limiting factor.

[4] The oligotrophic Lake Tanganyika is a lacustrine system which is located in the African Rift Valley and seems to be well suited for a biogeochemical study of the anaerobic oxidation of CH_4. This lake contains the largest anoxic freshwater body in the world, storing approximately 23 Tg of CH_4 gas below a permanent thermal stratification [***Hecky*, 1991**]. For comparison, ~90 Tg of CH_4 are stored in the Black Sea, the world's largest marine anoxic basin [***Reeburgh et al.*, 1991**]. Furthermore, water column sulphate concentrations are substantial and allow the formation of a chemically appropriate environment for the anaerobic oxidation of CH_4. In Lake Tanganyika, mixing processes and currents have intensively been investigated in the surface waters [***Naithani et al.*, 2007**; ***Gourgue et al.*, 2007a**; ***Podsetchine et al.*, 1999**]. Deep water renewal and vertical transport in the hypolimnion, however, have not been investigated although these processes are important for understanding the vertical distribution of dissolved substances.

[5] In the present study, the factors controlling CH_4 concentrations and oxidation in Lake Tanganyika were investigated by using a one-dimensional vertical advection-diffusion reaction model. Our hypothesis is that the anaerobic oxidation of CH_4 essentially controls CH_4 concentrations in stratified lakes that contain large bodies of anoxic water and sufficient amounts of sulphate, like Lake Tanganyika. The model was applied to evaluate the major

transport processes occurring in the thermocline and anoxic deep water body of Lake Tanganyika. Advective deep water renewal and turbulent mixing were estimated by inverse simulation of temperature, ^{3}H and CFC-12 concentrations, similar to an earlier study in Lake Baikal [***Peeters et al.*, 2000**]. The model was further used to outline the relevance of turbulent diffusion for vertical CH_4, O_2, and SO_4^{2-} transport and depletion. Model results were compared with the stable C isotopic composition of dissolved CH_4 and the abundance of archaea and aerobic methanotrophs with depth. Overall, these data provide evidence that the anaerobic oxidation of CH_4 is an important mechanism controlling the removal of CH_4 from the water column.

2. Methods

2.1. Sampling and Analysis

[6] Water column samples were taken for geochemical and microbiological investigations at station 1 in the northern basin and at station 2 in the southern basin (**Figure 1**) from aboard the R/V *Maman Benita*. Geochemical samples were collected in July 2001, 2002, and 2003, i.e., during dry monsoonal winters, and in January 2004, i.e., during wet summer, and microbiological samples were collected in July 2003 and in January 2004. Previous to sampling, vertical profiles of conductivity and temperature were recorded at both stations. Subsequently, water samples were collected with Niskin bottles.

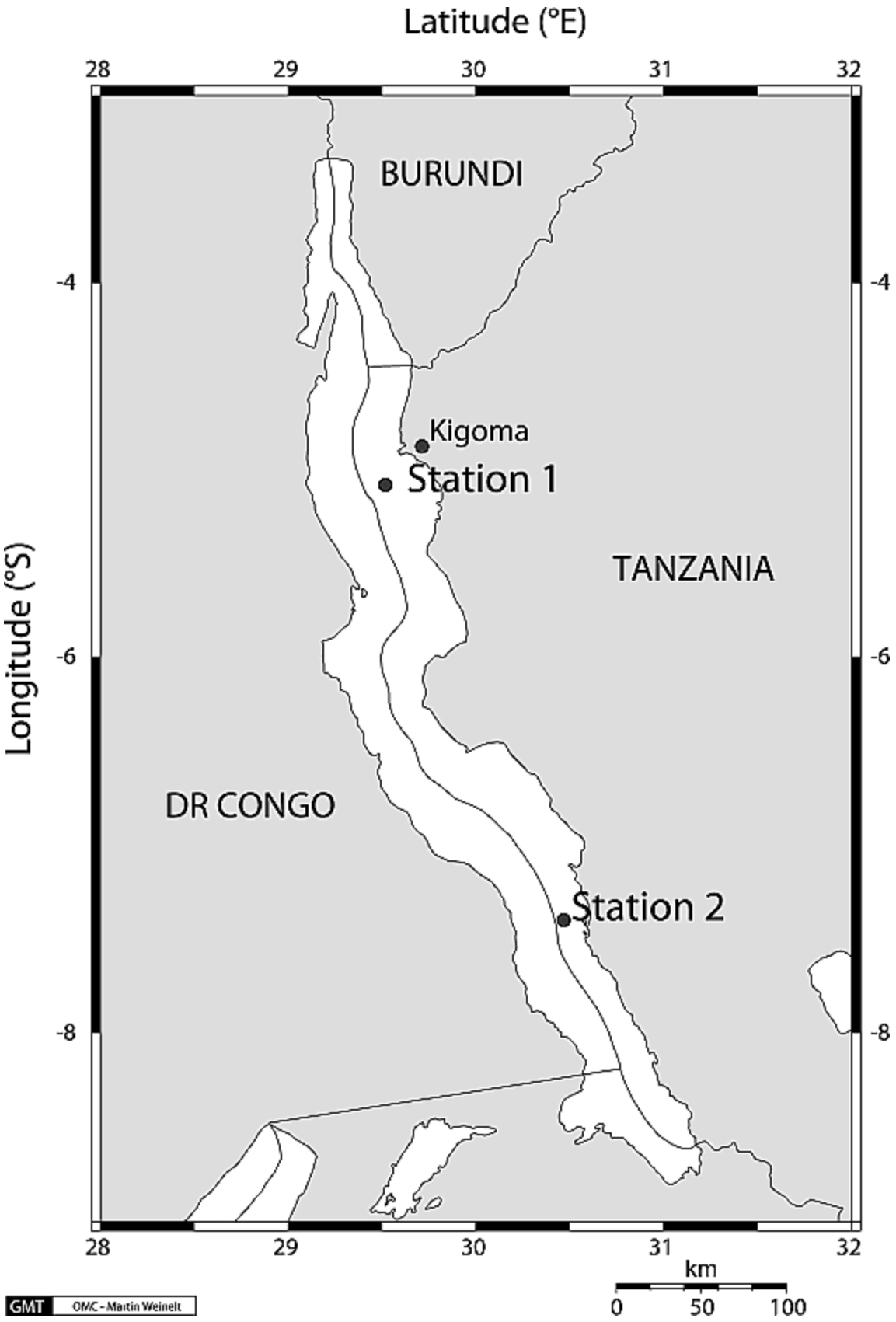
Latitude (°E)
28
29
30
31
32
BURUNDI
-4
Kigoma
Station 1
TANZANIA
Longitude (°S)
-6
DR CONGO
Station 2
-8
km
0
50
100
GMT
OMC - Martin Weinelt

Figure 1

Open in figure viewerPowerPoint

Map of Lake Tanganyika. Station 1 (5°05′S, 29°31′E, 1100 m water depth) is located in the northern basin (max. depth of 1310 m) and station 2 (7°24′S, 30°28′E, 1300 m water depth) in the southern basin (maximum depth of 1450 m). The map was created by using online map creation (OMC) by M. Weinelt (http://www.planiglobe.com/omc_set.html).

[7] For measuring CH_4 concentrations and stable carbon (C) isotopic ratios, water was filled into 120 mL serum bottles, poisoned with 5 mL NaOH or 50 μL of 50 mM $HgCl_2$ solution, respectively, and stored gas tight at 5°C. A 20 mL helium headspace was introduced and the samples equilibrated at 30°C for 4 h. Quantification of CH_4 was accomplished by injecting 200 μL of headspace from the serum vials into a Carlo Erba HRGC 5160 gas chromatograph equipped with a J&W GSQ column (30 m × 0.53 mm). Injection temperature was 70°C, FID temperature was 200°C, and the oven temperature was held at 40°C.

[8] The $\delta^{13}C$ signature of dissolved CH_4 was measured on an Isoprime isotope ratio mass spectrometer linked to a Trace Gas Preconcentrator (GV Instruments). The oxidation of CH_4 to CO_2 was performed by copper oxide (CuO) at 950°C. Isotopic compositions are reported in δ notation relative to the PeeDee Belemnite (VPDB) (Vienna, IAOA), determined by comparison with a 1% CH_4 lab standard of known isotopic composition relative to the VPDB standard. The reproducibility of analysis is ±0.8‰, and for CH_4 concentrations <1 μM it is ~2‰.

[9] Water for dissolved oxygen analyses was filled without any bubbles in Winkler flasks and for ammonium, nitrate, sulphate, and sulphide analyses in muffled 100 mL glass bottles. All samples were immediately measured aboard ship. Dissolved oxygen concentrations were measured using the Winkler titration method [***Grasshof*, 1983**]. Ammonium, nitrate, sulphate, and sulphide concentrations were determined colorimetrically [***DEW*, 2004**].

[10] For measuring bacterial abundance and investigating the microbial consortium by fluorescence in situ Hybridization (FISH) water was collected in muffled 50 mL glass bottles and killed with formaldehyde (2%). Preserved water samples (50 mL) were filtered using polycarbonate filters (0.2 μm pore size, 25 mm diameter, Millipore) and stored frozen at −20°C. Cell abundance was determined by epifluorescence microscopy (Zeiss Axioscope HBO50, 1000 magnification) of DAPI-stained cells [***Porter and Feig*, 1980**]. FISH was performed on the filters [***Pernthaler et al.*, 2002**], using CY3- and fluorescein-labeled 16SrRNA-targeted oligonucleotide probes (MWG Biotech AG, Switzerland): ARCH915 (5′-GTGCTCCCCCGCCAATTCCT-3′) [***Amann et al.*, 1990**; ***Pernthaler et al.*, 2002**], type I (M□84/M□705: 3′-

AGCCCGCGACTGCTCACC-5′/3′-CTAGACTTCCTTGTGGTC-5′) and type II (M□450: 3′-CTATTACTGCCATGGACCTA-5′) methanotrophs [***Eller et al.*, 2001**]. After testing for their specificity at ~60% v/v formamide, probes for archaea were hybridized at 40% and for bacteria at 20% formamide.

[11] The transient tracers ^{3}H and CFC-12 were sampled on a previous cruise in September 1998. Water samples were collected with Niskin bottles in the southern basin at station 2. The water was filled into copper tubes and locked gas tight. Tritium concentrations were determined by measuring the increase in helium concentration in previously degassed samples using mass spectrometry [***Beyerle et al.*, 2000**]. Concentrations of CFC-12 were measured with a gas chromatograph (Shimadzu GC-14 A) equipped with an electron capture detector and following the technique of ***Hofer and Imboden* [1998]**. The error in concentrations (at the 1 σ level) were estimated to be ±0.1 TU for ^{3}H (1 TU = 0.2488×10^{-14} mL STP g^{-1}) and ±5% for CFC-12.

2.2. Model Setup

[12] A one-dimensional vertical advection-diffusion-reaction model was implemented using the lake module of the software AQUASIM 2.1 [***Reichert*, 1994**, **1998**], which was developed to simulate various aquatic systems, like wastewater treatment plants, rivers, and particularly lakes [e.g., ***Peeters et al.*, 2000**; ***Omlin et al.*, 2001**; ***Schmid et al.*, 2006**; ***Matzinger et al.*, 2007**]. The software comprises tools for parameter estimation and sensitivity analysis. Partial differential equations for the processes included are solved by discretization of spatial derivatives, and subsequent implicit integration of the remaining system of coupled ordinary differential equations with variable time steps and variable integration order [***Petzold*, 1983**]. Vertical transport processes in the model include turbulent diffusivity which varies as a function of depth and advective transport caused by lateral inflows (i.e., deep water renewal). Masses of dissolved substances are conserved. A one-dimensional vertical grid with a resolution of 5 m was used for the model.

[13] The area of Lake Tanganyika, as a function of depth, was derived from an xyz data set produced by E. Deleersnijder (personal communication, 2007) based on the bathymetric map by ***Capart* [1949]**. The surface area is 32900 km^2. The water column was divided into the mixed surface layer (0–90 m, volume 2750 km^3), the thermocline (90–300 m, volume 5260 km^3), and the deep water (below 300 m, volume 11300 km^3). The three basins of Lake Tanganyika (northern, intermediate, and southern) are separated by sills of an approximate depth of 700 m [***Coulter and Tiercelin*, 1991**]. Although the simulation of the lake as a single basin represents a simplification, we argue that the major processes of interest were observed above 700 m depth.

The water column was divided into the mixed surface layer (0–90 m), the thermocline (90–300 m), and the deep water (below 300 m). The thickness of the surface layer was defined by the typical maximum depth reached by seasonal mixing during the dry season [***Gourgue et al.*, 2007b**]. The depth separating the thermocline and the deep water (300 m) was chosen based on observed profiles of temperature and dissolved constituents from the southern basin (**Figures 2**, **3**, and **4**).

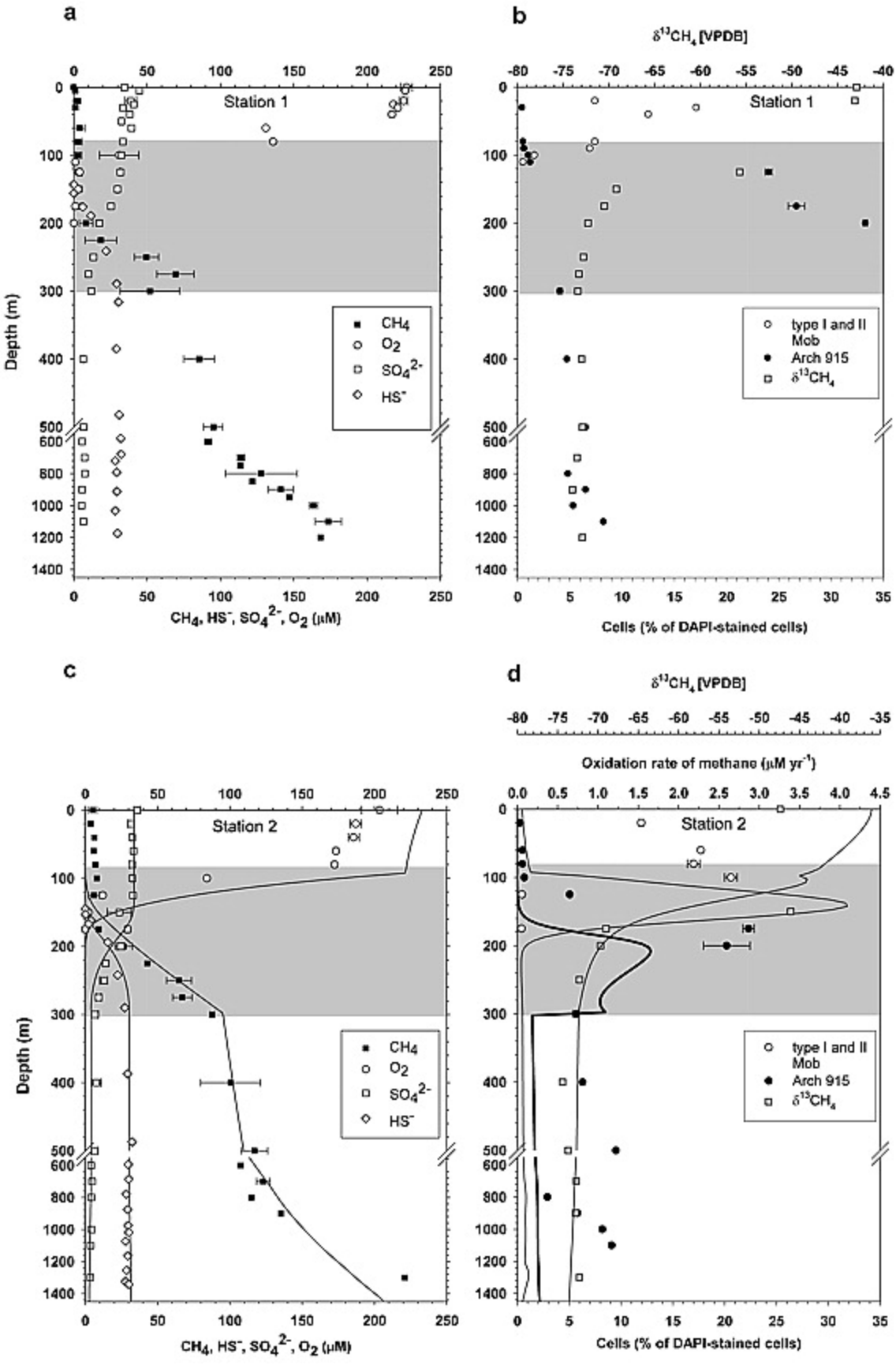
a
b
c
d
Station 1
Station 2
Depth (m)
CH4
O2
SO4 2-
HS-
CH4, HS-, SO4 2-, O2 (µM)
δ13CH4 [VPDB]
type I and II Mob
Arch 915
δ13CH4
Cells (% of DAPI-stained cells)
Oxidation rate of methane (µM yr-1)

Figure 2

Open in figure viewerPowerPoint

Chemical zoning and distribution of methanotrophy indicators (Figures 2a and 2c) and of cells and oxidation rates of methane (Figures 2b and d) across the Lake Tanganyika thermocline and anoxic regime at (a and b) station 1 and (c and d) station 2. Average (±2 SE) concentrations of CH_4, O_2, and HS^- from 2001, 2002, 2003, and 2004, and stable C isotope ratios of dissolved CH_4 ($\delta^{13}C$[VPDB]) from 2004 are presented. Concentrations of HS^- were taken from *Edmond et al.* [1993] because our data scattered considerably. Solid lines (Figure 2c) represent modeled data. Average percentages (±% mean deviation) of archaea (ARCH915) and type I and II methanotrophs (Mob) of DAPI-stained cells from 2003 and 2004 are shown. The solid thin line (Figure 2d) represents model-derived aerobic and the solid bold line (Figure 2d) model-derived anaerobic oxidation rates of methane. The thermocline zone is indicated by shading.

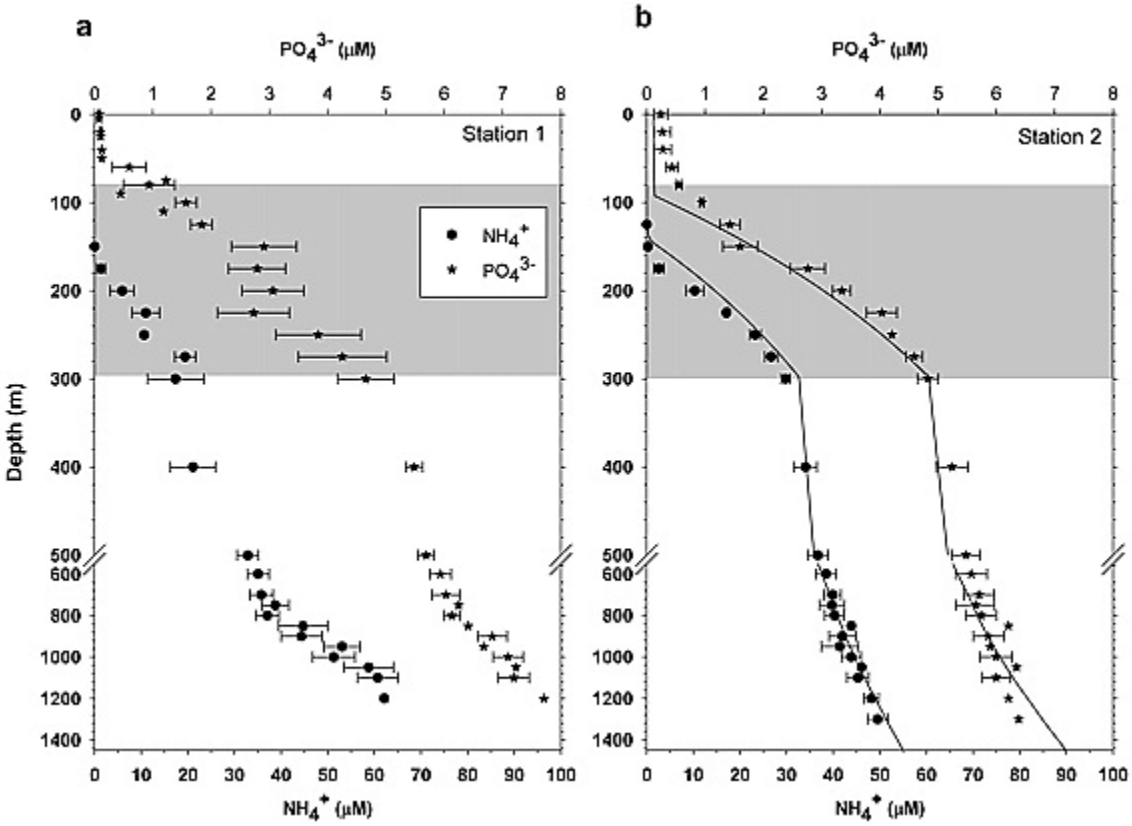

Figure 3

Open in figure viewerPowerPoint

Observed (symbols) and simulated (solid line) NH_4^+ and PO_4^{3-} concentrations in the water column of the (a) northern basin and (b) southern basin.

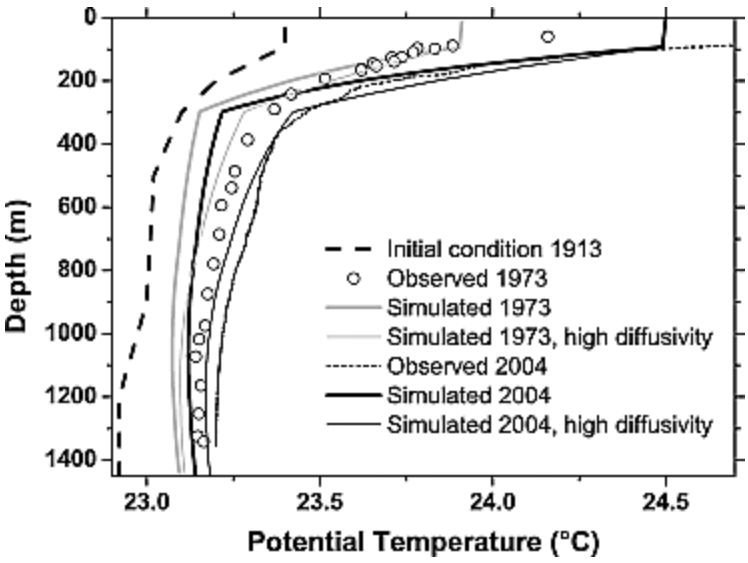

Figure 4

Open in figure viewerPowerPoint

Potential temperature in the water column of Lake Tanganyika: initial condition (year 1913) and observed and simulated values for the years 1973 and 2004 with standard diffusivity and diffusivity in the thermocline increased by a factor of 2 from 1.0×10^{-5} m^2 s^{-1} to 2.0×10^{-5} m^2 s^{-1}. The simulations correspond to temperature profiles during seasonal mixing and therefore are not expected to agree with observations in the mixolimnion.

[14] Simulations were started in the year 1913 und run until 2004, with a variable time step chosen by the integration algorithm of AQUASIM 2.1, which is based on stability criteria for the solution. The maximum time step was set to 0.1 years. Table 1 lists values and source references for the external forcing and the major model parameters. Air temperature and humidity values typical for the dry season (winter) were chosen, because they are representative for the time of the year when the surface layer is mixed. An additional simulation with seasonally varying forcing was run within the 'sensitivity analysis' (see below).

Table 1. Major Model and External Forcing Parameters

Parameter	Abbreviation	Value	Unit	Source
^{13}C fractionation factor for aerobic oxidation of CH_4	$\alpha_{CH4,aer}$	0.98	-	*Whiticar* [1999]

Parameter	Abbreviation	Value	Unit	Source
^{13}C fractionation factor for anaerobic oxidation of CH_4	$\alpha_{CH4,anaer}$	0.995	-	*Whiticar* [1999]
^{13}C fractionation factor for gas exchange at the lake surface	$\alpha_{CH4,gas}$	0.9992	-	*Knox et al.* [1992]
Vertical turbulent diffusivity in the deep water (below 300 m depth)	$K_{Z,deep}$	1.0×10^{-4}	$m^2\ s^{-1}$	estimated parameter
Vertical turbulent diffusivity in the thermocline (between 90 and 300 m depth)	$K_{Z,thermo}$	1.0×10^{-5}	$m^2\ s^{-1}$	estimated parameter
Vertical turbulent diffusivity in the mixolimnion	$K_{Z,mix}$	1.0×10^{-3}	$m^2\ s^{-1}$	estimated parameter
Deep water renewal rate (below 90 m depth)	Q_{deep}	35	$km^3\ yr^{-1}$	estimated parameter
Geothermal heat flux	F_{geo}	0.05	$W\ m^{-2}$	*Pollack et al.* [1993]
Areal release of CH_4 from sediment	$r_{CH4,sed}$	0.5	Mol $m^{-2}\ yr^{-1}$	estimated parameter
Areal release of NH_4 from sediment	$r_{NH4,sed}$	0.09	Mol $m^{-2}\ yr^{-1}$	estimated parameter
Areal release of PO_4^{3-} from sediment	$r_{PO4,sed}$	0.01	Mol $m^{-2}\ yr^{-1}$	estimated parameter
Oxidation rate of H_2S with O_2	$k_{Ox,H2S}$	0.16	(μmol	*Wang and Van Cappellen* [1996]

Parameter	Abbreviation	Value	Unit	Source
			$L^{-1})^{-1}$ yr^{-1}	
Rate of aerobic oxidation of CH_4	$k_{Ox,CH4,aer}$	0.02	(μmol $L^{-1})^{-1}$ yr^{-1}	estimated parameter
Rate of anaerobic oxidation of CH_4 in the thermocline	$k_{Ox,CH4,anaer,thermo}$	0.003	(μmol $L^{-1})^{-1}$ yr^{-1}	estimated parameter
Rate of anaerobic oxidation of CH_4 in the deep water	$k_{Ox,CH4,anaer,deep}$	0.0004	(μmol $L^{-1})^{-1}$ yr^{-1}	estimated parameter
Half saturation constant for limitation of anaerobic oxidation of CH_4 by O_2	K_{O2_CH4}	1	μmol L^{-1}	tentative, order of magnitude as for anammox bacteria [*Strous and Jetten*, 2004]
First-order consumption rate of oxygen	k_{O2}	0.2	yr^{-1}	estimated parameter
First-order consumption rate of PO_4^{3-} above 40 m depth	k_{PO4}	2	yr^{-1}	estimated parameter
First-order consumption rate of NH_4^+ above 150 m depth	k_{NH4}	10	yr^{-1}	arbitrary
Isotopic signature $\delta^{13}C$ of CH4 released from mineralization	$\delta^{13}C_{CH4,sed}$	−75	‰	estimated parameter
Precipitation	Q_P	35.5	km^3 yr^{-1}	*Branchu and Bergonzini* [2004][a]
Evaporation	Q_E	55.3	km^3 yr^{-1}	*Branchu and Bergonzini* [2004][b]

Parameter	Abbreviation	Value	Unit	Source
Inflows	Q_p	29.5	$km^3\ yr^{-1}$	*Branchu and Bergonzini* [2004][c]
Wind speed	v_{wind}	3	$m\ s^{-1}$	*O'Reilly et al.* [2003]
Relative humidity during the dry season	h_r	60	%	*Spigel and Coulter* [1996]

- a Other estimates are 35 $km^3\ yr^{-1}$ [*Spigel and Coulter*, 1996] and 42.8 $km^3\ yr^{-1}$ [*Nicholson and Yin*, 2004].
- b Other estimates are 50 $km^3\ yr^{-1}$ [*Spigel and Coulter*, 1996] and 56.5 $km^3\ yr^{-1}$ [*Nicholson and Yin*, 2004].
- c Other estimate is 18 $km^3\ yr^{-1}$ [*Spigel and Coulter*, 1996].

[15] Average concentrations of CH_4, O_2, SO_4^{2-}, HS^-, PO_4^{3-}, and NH_4^+, and the stable C isotopic ratio of dissolved CH_4 ($\delta^{13}CH_4$) in the southern basin (**Figures 2c** and **3b**) represented initial conditions in the lake's water column. For HS^-, the profile measured by ***Edmond et al.* [1993]** in the southern basin was used, since our own measurements scattered considerably. Observations from the northern basin were not used for simulations, but are shown in some figures for comparison (**Figures 2a** and **3a**). Steady state conditions were assumed for all tracers in Lake Tanganyika except for temperature and the transient tracers CFC-12 and ^3H. Temperature has been increasing in Lake Tanganyika during the last 100 years. The vertical profile from ***Stappers* [1913]**, as presented by ***Verburg and Hecky* [2009]**, was used to represent the initial condition (**Figure 4**). All observed in situ temperatures were converted to potential temperatures by subtracting an average adiabatic temperature gradient of 1.75×10^{-4} °C m^{-1}.

[16] Time-varying atmospheric concentrations of CFC-12 were represented by average observed concentrations from the Southern hemisphere [***Walker et al.*, 2000**]. Solubility in water was calculated by using the constants of ***Warner and Weiss* [1985]**. The CFC-12 concentrations in riverine inflows were assumed to be in equilibrium with the atmosphere. In addition to our ^3H data, one profile of ^3H concentrations was available from measurements performed in the northern basin in 1973 [***Craig*, 1975**]. Tritium concentrations in rain and riverine inflows were set to the average of concentrations observed at stations within the GNIP network [***International Atomic Energy Agency/World Meteorological Organization*, 2006**] located nearby (Entebbe, Muguga, Makutapora, Kericho, Dar es Salaam, Ndola, Harare).

[17] Gas exchange (for CFC-12, CH_4, and O_2) between the surface of the lake and the atmosphere was calculated according to

$$F_C = v_{gas}\left(C_{equ} - C_{surf}\right) \quad (1)$$

The flux F_c between the lake surface and the atmosphere was equal to the product of the gas exchange velocity v_{gas} and the difference between the equilibrium C_{equ} and the actual concentration at the surface C_{surf}. The gas exchange velocity for a Schmidt number of 600 (Sc = 600) was calculated according to equation (5) of *Cole and Caraco* [1998]. The exchange velocities of the different gases were corrected for the Schmidt numbers of the respective gases using

$$v_{gas} = v_{gas,600}(600/Sc)^n \quad (2)$$

with n = 2/3. The Schmidt numbers of the different gases were calculated as a function of temperature using the polynoms given by *Wanninkhof* [1992].

[18] The exchange of ^3H between the lake and the atmosphere was calculated using the equations given by *Imboden et al.* [1977]. The surface input of ^3H is given by

$$F_{3H} = E\frac{\alpha\left(C_{surf} - hC_{rain}\right)}{1-h} \quad (3)$$

in which E represents the evaporation, α the equilibrium fractionation between water and air, h the relative humidity of the air at the water surface temperature, C_{surf} the concentration at the surface, and C_{rain} the observed concentrations in rainwater [*Aeschbach-Hertig*, 1994; *Imboden et al.*, 1977]. Because the difference between air and surface water temperatures was generally small in Lake Tanganyika, relative humidity values from the air were regarded representative for h. Tritium was simulated to decay in the water column with a decay constant of 0.05626 yr^{-1}, corresponding to a half-life time of 12.32 years [*Lucas and Unterweger*, 2000].

[19] The vertical turbulent diffusivity in the surface layer is set to a value such that the water age, defined in the model as the time since the last contact with the lake surface, is on average 1 year in the mixolimnion. This requires a diffusivity of 1×10^{-3} m^2 s^{-1}.

[20] In order to simulate CH_4 concentrations in the lake, the gas exchange process described above and the following processes were included in the model (**Table 2**): release of CH_4 from the sediment (proportional to the sediment area at each depth), aerobic and anaerobic oxidation of methane, oxidation of HS^- to SO_4^{2-}, and volumetric consumption of O_2. In order to keep SO_4^{2-} concentrations constant in the surface layer, SO_4^{2-} concentrations in the riverine inflows were set to 10 μM. This equals the average observed concentrations [***Langenberg et al.*, 2003**], except for the River Ruzizi, which exhibits an average SO_4^{2-} concentration of 124 μM and contributes 5.4 km^3 yr^{-1} to the total river inflow, i.e., ~600 mmol yr^{-1} more than included in the

model. We conclude that there must be an additional sink of ~20 mmol SO_4^{2-} m^{-2} yr^{-1} from the mixolimnion, which is not explicitly represented by a process in the model.

Table 2. Geochemical Processes Included in the Model

Process	Process Rate	Stoichiometric Coefficients					
		CH_4[a]	SO_4^{2-}	HS^-	O_2	NH_4^+	PO_4^{3-}
Anaerobic decomposition of organic material[b]	$r_{CH4,sed} \times dA/dz \times (1/A)$	1	-	-	-	0.18	0.02
Aerobic oxidation of CH_4	$k_{Ox,CH4,aer} \times [O_2] \times [CH_4]$	−1	-	-	−2	-	-
Anaerobic oxidation of CH_4[c]	$k_{Ox,CH4,anaer} \times [SO_4] \times [CH_4] \times (1 - [O_2]/(K_{O2\_CH4} + [O_2]))$	−1	−1	1	-	-	-
HS^- oxidation	$k_{Ox,H2S} \times [HS^-] \times [O_2]$	-	1	−1	−2	-	-
O_2 consumption	$k_{O2} \times [O_2]$	-	-	-	−1	-	-
NH_4^+ consumption[d]	$k_{NH4} \times [NH_4^+]$	-	-	-	-	−1	-
PO_4^{3-} consumption[e]	$k_{PO4} \times [PO_4^{3-}]$	-	-	-	-	-	−1

- a All processes influencing CH_4 were separately simulated for the heavier C isotope ($^{13}CH_4$), using the fractionation factors and the isotopic signature of the CH_4 from organic material given in Table 1.
- b Released from sediments proportional to sediment area, only below 90 m depth.
- c Different reaction rate constants were used in the thermocline and in the deep water (Table 1).
- d Only above 150 m depth, arbitrary rate with the aim of quickly removing NH_4^+.
- e Only above 40 m depth, rate set to reach concentrations comparable to observations.

[21] The $\delta^{13}CH_4$ values were calculated based on the following assumptions: The $\delta^{13}C$ of CH_4 released from the sediment was estimated in order to fit the simulated $\delta^{13}C$ in the deep water to the observed values. The fractionation factors α were set to 0.98 (i.e., the reaction is 0.98 times as fast for $^{13}CH_4$ as for $^{12}CH_4$) for aerobic oxidation of CH_4 and to 0.995 for anaerobic oxidation of CH_4, both in the range of those cited by ***Whiticar* [1999]**. For gas exchange at the lake surface, a fractionation factor of 0.9992 was used [***Knox et al.*, 1992**].

[22] In a first step, the model was used to estimate the relevant parameters for vertical transport (vertical turbulent diffusivities and deep water renewal rates) based on transient tracers and temperature profiles. Then, concentrations of the nutrients NH_4^+ and PO_4^{3-} were simulated with the transport parameters obtained from the inverse fitting of the transient tracers to validate the parameterization of the transport processes. Finally, the validated transport model was extended by including biogeochemical processes, and the implications of these processes on CH_4 concentrations in the lake were investigated.

3. Results

3.1. Observed Water Column Concentrations of O_2, CH_4, SO_4^{2-}, HS^-, NH_4^+, PO_4^{3-}, and $\delta^{13}CH_4$ Values

[23] Average measured concentrations (μM ± standard error, SE, if n = 3) from water samples of the northern and southern basin are presented in **Figures 2** and **3**. In the northern basin, the deep water below ~200 m depth was permanently anoxic, and CH_4 concentrations were ~170 μM at 1200 m, ~8 μM at 200 m depth, and ~0.1 μM at the surface. In the southern basin, water column profiles were comparable to the deep northern basin (~220 μM at 1200 m, ~27 μM at 200 m depth, and ~5 μM at the surface) (**Figures 2a and 2c**). In the northern basin, the $\delta^{13}CH_4$ values were fairly homogenous below ~200 m depth (−72‰), however, within the thermocline CH_4 was heavier, and −43‰ at the surface. Note, the $\delta^{13}C$ of atmospheric CH_4 is −47‰ [***Stevens and Wahlen*, 2000**]. In the southern basin, the $\delta^{13}CH_4$ value was fairly homogeneous below and above the thermocline, while within it sharply shifted from −70‰ to −46‰. Sulphate, a possible electron acceptor for the anaerobic oxidation of CH_4, ranged between 30 and 36 μM in the surface water of both basins and showed a sharp decrease at ~200 m depth and below, while HS^- appeared in the thermocline and concentrations were high (>50 μM) below. However, the HS^- data were strongly scattered (data not shown), and therefore the data by ***Edmond et al.* [1993]** from the southern basin were used for model simulations. Ammonium concentrations were highest in deep water (50 to 60 μM) and the sharpest upward decrease occurred between

300 and 150 m depth in both basins (**Figure 3**). Similarly, PO_4^{3-} concentrations were highest in deep water (6 to 8 μM) and concentrations strongly decreased between 300 and 80 m depth in both basins.

3.2. Cell Abundance and FISH

[24] We detected numerous single cells from water column samples with gene probes specific for the domains archaea and bacteria using FISH. In both basins, an increase of the abundance of archaea (up to ~33% of total DAPI-stained cells in the northern basin) was identified in the thermocline (**Figures 2b and 2d**). The archaeal cells were well recognized by DAPI stain and probe signal. About 12 to 17% of all DAPI-stained cells within 30 to 40 m depth in the northern and 19 to 22% at 100 m depth in the southern basin were identified to belong to type I and II methanotrophs. Type I methanotrophs dominated by up to 95%.

3.3. Diffusivity, Temperature, and Deep Water Renewal

[25] Below 400 m depth, the transient tracers CFC-12 and ^{3}H were observed at significant concentrations, with a considerable scatter, but no clear depth trend. In principle, there are two possibilities to explain these concentrations: (1) very high vertical turbulent diffusivities or (2) an advective transport of surface water to the deep water. The former contradicts both the observed gradients of other constituents in the deep water, and a first-order estimate of the diffusivity in the thermocline of $\leq 10^{-5}$ m^2 s^{-1}, which was based on the vertical density stratification and the energy input from the wind using the method described by ***Wüest et al.* [2000]**.

[26] For this reason, the volume flow of deep water renewal in the thermocline between 90 to 350 m depth was optimized to fit the observed water column concentrations of CFC-12 and ^{3}H (**Figure 5**). For ^{3}H and CFC-12, zero concentrations were assumed as initial conditions for the year 1904. Then, the model was run until the years 1973 [***Craig*, 1975**]) and 1998, when concentrations were measured.

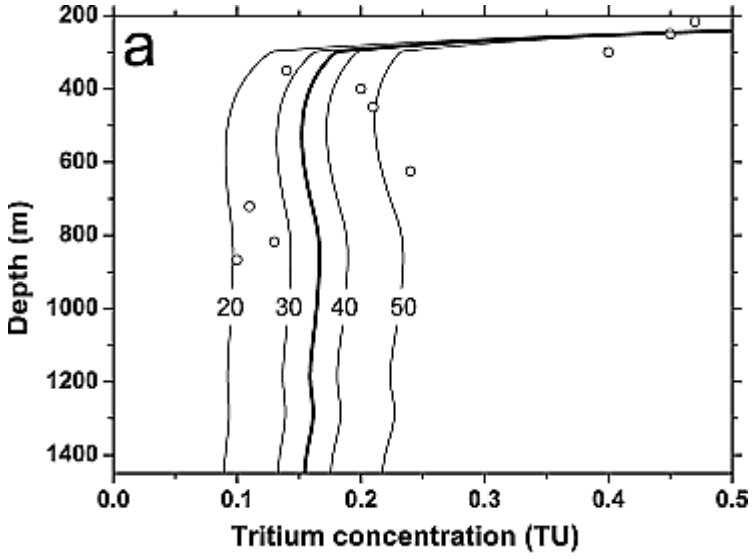
a
Depth (m)
200
400
600
800
1000
1200
1400
20
30
40
50
0.0
0.1
0.2
0.3
0.4
0.5
Tritium concentration (TU)

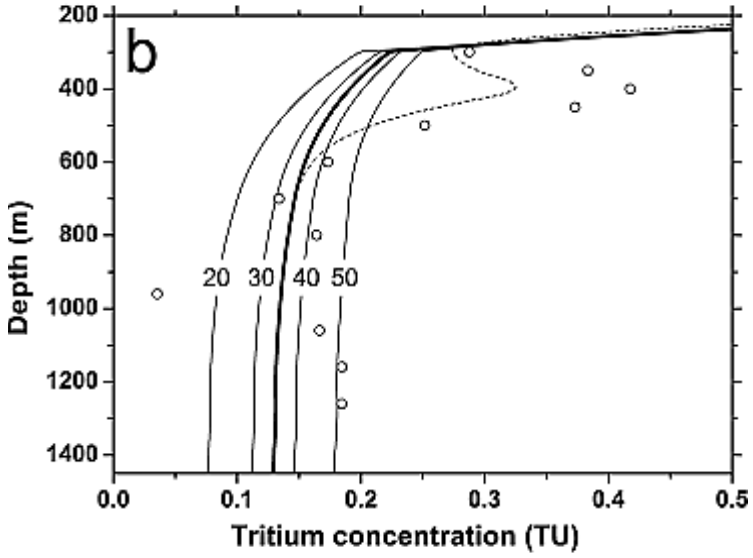
b
Depth (m)
200
400
600
800
1000
1200
1400
20
30
40
50
0.0
0.1
0.2
0.3
0.4
0.5
Tritium concentration (TU)

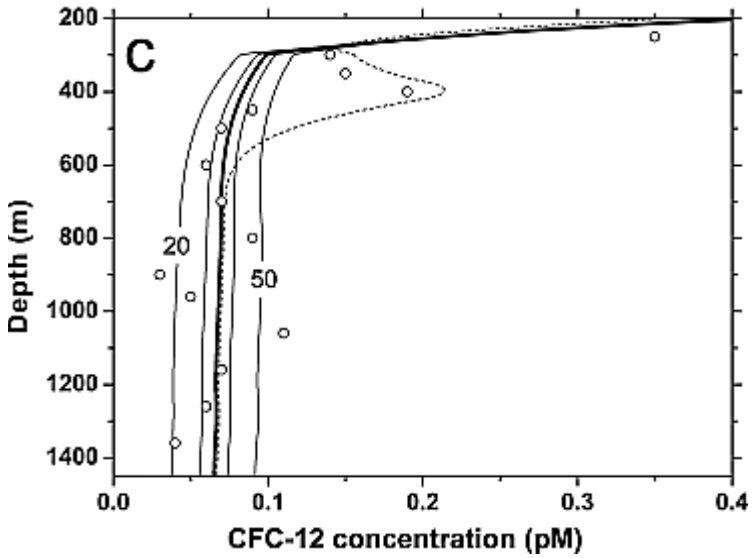
c
Depth (m)
200
400
600
800
1000
1200
1400
20
50
0.0
0.1
0.2
0.3
0.4
CFC-12 concentration (pM)

Figure 5

Open in figure viewerPowerPoint

Observed concentrations (circles) in the deep water of Lake Tanganyika compared to simulations (lines) for different deep water renewal rates of (a) ^{3}H in 1973, (b) ^{3}H in 1998, and (c) CFC-12 in 1998. Volume flows (km^3 yr^{-1}) are indicated by numbers on the lines. The thick lines indicate the standard simulation with a flow of 35 km^3 yr^{-1}; the thin dashed lines represent a simulation with an additional surface water input of 300 km^3 at 400 m depth during the previous year.

[27] It is assumed that the deep water is formed by plunging surface water due to differential cooling in shallower areas of the lake [***Verburg and Hecky*, 2009**], similar to the processes described for Lake Issyk-Kul [***Peeters et al.*, 2003**]. The vertical depth distribution of the deep water new formation is unknown. Several different distributions were tested, and the most consistent results were achieved by assuming a formation rate that decreases linearly from 90 m depth to the deepest point of the lake. Least squares fitting to the observed concentrations of ^{3}H (1973 and 1998) and CFC-12 (1998) below 400 m depth resulted in consistent deep water renewal rates below 90 depth of 37.4 km^3 yr^{-1} and 32.5 km^3 yr^{-1}, respectively. In reality, the deep water renewal is a highly dynamic process and it must be assumed that both the quantity and the depth distribution vary significantly from year to year. For further calculations, a constant deep water renewal rate of 35 km^3 yr^{-1} was assumed below 90 m depth, of which 24 km^3 yr^{-1} are discharged below 300 m depth. Concentrations of CH_4, HS^-, SO_4^{2-}, O_2, CFC-12, and ^{3}H in the deep water inflow were set equal to concentrations at 10 m depth.

[28] The vertical temperature profiles in the thermocline follow exponential curves. This would be expected in case of a constant diffusivity combined with upwards advection driven by deep water renewal. By fitting an exponential curve to the observed profiles, the ratio of the turbulent diffusivity to the uplift velocity caused by deep water renewal rate can be estimated. The resulting diffusivity in the thermocline is 6×10^{-6} m^2 s^{-1}, in agreement with the first-order estimate based on the method of ***Wüest et al.* [2000]**. The diffusivity in the thermocline can also be optimized in order to reproduce the observed temperature increase over time [***Verburg and Hecky*, 2009**]. This requires several assumptions: we assumed that the water propagating downward in the deep water renewal process is slightly (0.1°C) colder than the ambient water at the depth where it intrudes and stratifies, that the geothermal heat flow corresponds to the average of the few available observations (0.5 W m^{-2} [***Pollack et al.*, 1993**]), and that there is no significant heating by warm springs, even though geothermal springs are entering the surface layer [***Tiercelin et al.*, 1993**]. Furthermore, it was assumed that the temperature at the base of the mixolimnion has been increasing by ~1°C within a century, namely from 23.5°C in 1900 to

23.9°C in 1975 and 24.5°C in 2000. A diffusivity value on the order of 2×10^{-5} m^2 s^{-1} would then be required in order to supply sufficient heat to the deep water (**Figure 4**). Based on this evaluation, the diffusivity in the thermocline was set to 1×10^{-5} m^2 s^{-1}. We estimate that this diffusivity should be correct within a factor of 2.

[29] The diffusivity in the deep water is less well constrained. Measured vertical profiles of NH_4^+ and PO_4^{3-} concentrations from 1975 [***Edmond et al.*, 1993**] and from 2002 to 2004 (data not shown) show very consistent gradients in the deep water, indicating that the chemical conditions in the deep water are near steady state. The average observed gradients of chemical compounds such as alkalinity, silica, NH_4^+ and PO_4^{3-}, in the deep water of the southern basin are typically by a factor of ~10 smaller compared to the thermocline. If we assume areal fluxes to be similar over depth, this indicates that the diffusivity in the deep water is about 10 times larger than in the thermocline. Hence, we tentatively set the diffusivity in the deep water to 1×10^{-4} m^2 s^{-1}.

[30] The observed profiles of the transient tracers CFC-12 and ^3H show two features that cannot be explained by the simple model approach (**Figure 5**). In 1998, elevated concentrations were observed at around 400 m depth, which would require a large intrusion event at this depth. Based on the estimated vertical diffusivity in the deep water of the lake, the width of the peak indicates an average age of the intrusion of approximately 1 year. An additional simulation was run with an individual inflow of 300 km^3 of water at 400 m depth during the year 1997 and is shown for comparison in **Figures 5b and 5c**. Such an intrusion could explain the observed concentrations of the transient tracers. It is unclear how well the peak would have been horizontally distributed across the whole lake within one year. The observed peaks could therefore also be interpreted as a rather local signal of a smaller intrusion or as a more distant signal of an even larger event in another basin. Negative peaks at around 900 m depth may suggest an inflow of old groundwater, which has not been in contact with the atmosphere for at least 50 years.

3.4. Simulation of Nutrient and Oxygen Concentrations

[31] In order to examine the assumptions for mixing derived above, concentrations of NH_4^+ and PO_4^{3-} were simulated. For both compounds it was assumed that they are released at a constant rate proportional to the sediment area at all depths. There are no data available from Lake Tanganyika to support this assumption. This would require measurements of sediment fluxes with sediment traps at different depths. However, in Lake Kivu, water column mineralization in the anoxic layer was shown to be negligible, and observed sediment fluxes were homogeneous with depth [***Pasche et al.*, 2010**]. In the model, NH_4^+ is quickly consumed by nitrification with an arbitrary fast rate at depths <150 m in order to keep mixolimnion concentrations at very low

levels, and PO_4^{3-} is consumed by primary production in the mixolimnion at a first order rate of 2 yr^{-1} to keep surface concentrations near typical observed levels of 0.1 μM. Areal release rates of ~0.09 mol NH_4^+ m^{-2} yr^{-1} and ~0.01 mol PO_4^{3-} m^{-2} yr^{-1} are required to keep the concentrations constant in the deep water. Simulated concentrations agree well with observations, supporting the assumptions for mixing processes made above (**Figure 3b**). It should be mentioned that, assuming a C:N:P ratio of 168:19:1 [***Järvinen et al.*, 1999**] of the mineralized organic matter, the release rates would correspond to a relatively low mineralization rate of ~10–20 g C m^{-2} yr^{-1} (comparable to that of ***Ramlal et al.* [2003]**). A first order volumetric oxygen consumption rate of 0.2 yr^{-1} was required to reproduce the observed vertical oxygen profile.

3.5. Production and Oxidation of Methane

[32] The observed concentrations could best be reproduced in steady state using an areal production of 0.5 mol CH_4 m^{-2} yr^{-1} (**Figure 2**). The estimated ratio of C:N:P of the mineralized organic matter, assuming a production of 50% CO_2 and 50% CH_4 during anaerobic decomposition, was 100:9:1. Compared to the average composition of the seston, P is enriched by a factor of almost 2 in the mineralized organic matter. This enrichment is at least partially due to seasonal effects. During the dry season, primary production peaks while N and P are enriched in the seston compared to the annual average [***Stenuite et al.*, 2007**]. Furthermore, it can be expected that a higher fraction of the freshly produced organic matter is exported from the epilimnion during the dry season than during the wet season when nutrients are more limiting and the stratification is more stable. The sedimenting and mineralized organic matter is therefore more representative of the organic matter produced during the dry season, as it has been observed using sediment traps in Lake Malawi [***Pilskaln*, 2004**]. The $\delta^{13}C$ of the produced CH_4 was set to −75 ‰ in order to agree with the observed $\delta^{13}C$ of the CH_4 in deep water (**Figure 2**). The CH_4 observed in the deep water is ~2 ‰ heavier because of the partial oxidation with O_2 and SO_4^{2-} supplied by the deep water renewal.

[33] The rates of the aerobic and anaerobic oxidation of CH_4 were adjusted to fit the observed gradients of CH_4, HS^-, and SO_4^{2-} with depth. It was not possible to reproduce both the gradient of CH_4 in the thermocline and the SO_4^{2-} concentrations in the deep water with the same reaction rate for anaerobic CH_4 oxidation. In reality, the supply of SO_4^{2-} by deep water renewal is intermittent, with varying depths and volumes of intrusions, contrary to the thermocline, where SO_4^{2-} is continuously supplied from the mixolimnion by turbulent diffusion, supporting the activity of a more ‘efficient’ population of anaerobically oxidizing CH_4 cells. Therefore we used different reaction rate constants for the anaerobic oxidation of CH_4 in the thermocline and the deep water

in the model. The reaction rate constants were estimated to 0.02 yr^{-1} ($\mu M\ O_2$)$^{-1}$ for the aerobic, and 0.003 and 0.0004 yr^{-1} ($\mu M\ SO_4^{2-}$)$^{-1}$ for the anaerobic oxidation of CH_4 in the thermocline and the deep water, respectively. These values correspond to 3 months residence time of CH_4 for aerobic oxidation at typical O_2 concentrations of 200 μM in the mixolimnion, and to about 20 and 600 years residence time of CH_4 for anaerobic oxidation at SO_4^{2-} concentrations present in the thermocline and the deep water, respectively. The effective residence time of CH_4 in the deep water in the model is on the order of 100 y, as it is transported upwards by uplift caused by deep water renewal and turbulent diffusion (**Figure 6**). The vertical structure of simulated oxidation rates agrees well with that of observed abundances of archaea (**Figure 2d**).

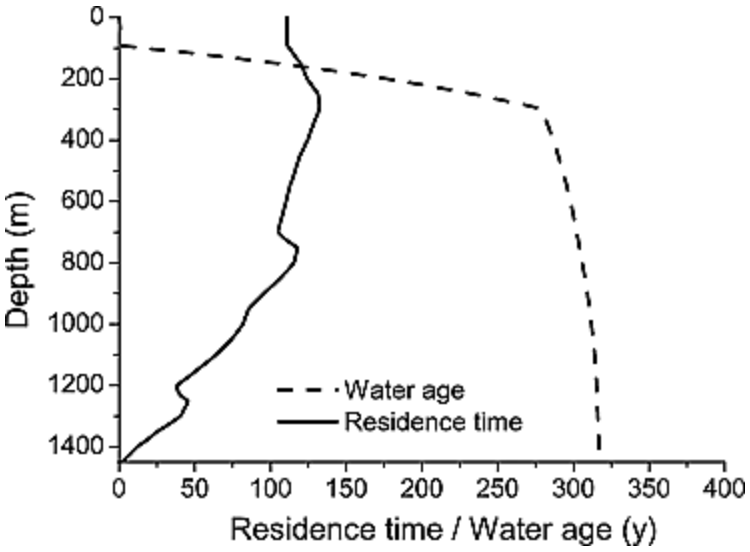

Figure 6

Open in figure viewerPowerPoint

Simulated average residence time of CH_4 (calculated as the stock below a given depth divided by the integrated production below this depth) and water age (average time since the last contact of the water with the atmosphere at the lake surface).

3.6. Sensitivity Analysis

[34] The sensitivity of the model in respect to the driving parameters was tested by the following additional simulations. A simulation including seasonal variability was calculated using the following external forcing: sine functions for relative humidity (average 0.75, amplitude 0.15), lake surface temperature (average increasing from 25°C in 1900 to 25.4°C in 1975 and 26°C in 2000, amplitude 2°C), evaporation (average 50 $km^3\ yr^{-1}$, amplitude 7 $km^3\ yr^{-1}$), precipitation (average 35 $km^3\ yr^{-1}$, amplitude 30 $km^3\ yr^{-1}$) and mixolimnion depth (90 m during 20% of the

year and 30 m during the other time). Lake surface temperature, precipitation, and humidity exhibit their maxima during the wet season, evaporation and mixing depth during the dry season. We found that effects of seasonality were small on the simulated depth distribution of reactants.

[35] The deep water renewal rate was varied in steps of 10 $km^3\ yr^{-1}$ from 20 to 50 $km^3\ yr^{-1}$. The impact of deep water renewal on concentrations of CH_4, SO_4^{2-}, HS^-, $\delta^{13}CH_4$, and the anaerobic oxidation of CH_4, is shown in **Figure 7**, and on ^3H and CFC-12 concentrations in **Figure 5**. Precipitation and evaporation were varied by ±5 $km^3\ yr^{-1}$, relative humidity by ±10%, and wind speeds of 1 and 6 $m\ s^{-1}$ were simulated. The most significant effects of changes in these parameters could be observed for simulated ^3H concentrations due to changes in humidity. A change in relative humidity by 10% resulted in a similar change in simulated ^3H concentrations, as if increasing the deep water renewal rate by about 10 $km^3\ yr^{-1}$.

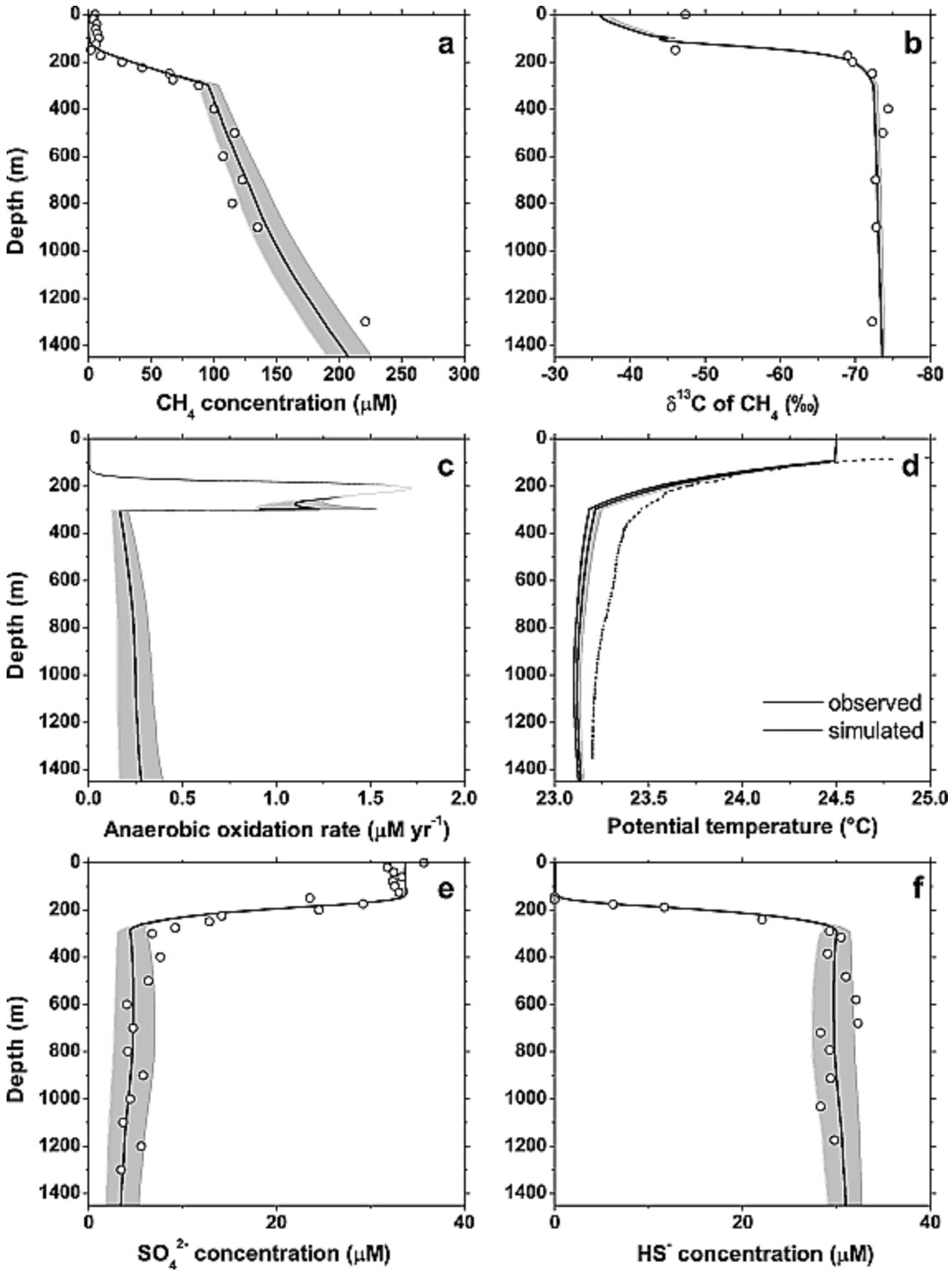

Figure 7

[Open in figure viewerPowerPoint]

Sensitivity of simulated vertical profiles of (a) CH_4 concentrations, (b) $\delta^{13}C$ of CH_4, (c) the rate of the anaerobic oxidation of CH_4, (d) potential temperature, (e) SO_4^{2-}, and (f) HS^- concentrations on the deep water renewal rate. The gray bands indicate the range of simulated results for a change of the renewal rate by ±10 $km^3\ yr^{-1}$. Open symbols represent measured concentrations, and the dashed line represents the temperature.

[36] The $\delta^{13}C$ of dissolved CH_4 produced in the sediment was varied by ±5‰. This change influenced $\delta^{13}CH_4$ values by the same amount in the whole water column. Fractionation factors were varied by ±0.01 for the aerobic fractionation and by ±0.002 for the anaerobic fractionation of CH_4. The former had a significant effect on $\delta^{13}CH_4$ values in the mixolimnion (although this is most probably strongly influenced by shallow sources). The latter caused a variation of about ±0.3‰ in the whole deep water.

[37] The aerobic oxidation rate of CH_4 was multiplied and divided by a factor of 10. A higher aerobic oxidation rate would mainly affect concentrations and the $\delta^{13}C$ of dissolved CH_4 in the mixolimnion. However, both are most probably strongly influenced by shallow CH_4 sources as well as by seasonal fluctuations, and can therefore not be used to calibrate this parameter with high accuracy without further information on shallow CH_4 sources.

[38] Finally it was tested whether the observed profiles of CH_4, SO_4^{2-}, and HS^- could also be reproduced using a model without anaerobic oxidation of methane. In order to achieve this, the following changes had to be made to the model: the diffusivity in the thermocline was increased by a factor of 2 to $2 \times 10^{-5}\ m^2\ s^{-1}$; an additional process was added that reduces SO_4^{2-}, and HS^- at approximately the same rate as this is done by the anaerobic oxidation of CH_4 in the base model; the CH_4 release rate from the sediment was slightly reduced to 0.4 $mmol\ m^{-2}\ yr^{-1}$; the first-order consumption rate of oxygen was increased to 0.5 yr^{-1}. With these adaptations of the model, observed CH_4 concentrations could be reproduced almost as well as with the base simulation (**Figure 8**).

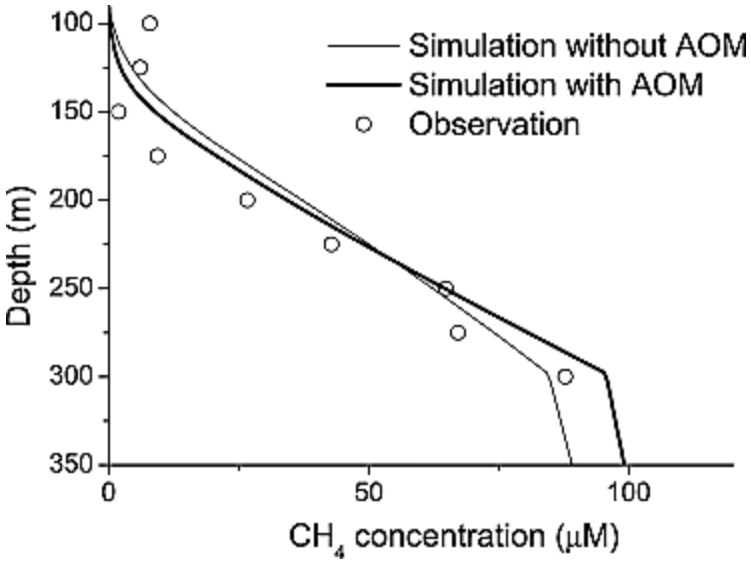

Figure 8

Open in figure viewerPowerPoint

Simulated concentrations of CH_4 in the thermocline in optimized model versions with and without the anaerobic oxidation of CH_4. The differences between the two models are described in section 3.6.

4. Discussion

[39] In Lake Tanganyika, high concentrations of dissolved CH_4 possibly originate from degradation of settling organic particles and 'relict' sediment organic C [***Craig*, 1975**; ***Hecky*, 1978**] under low SO_4^{2-} concentrations (≤25 μM) as compared to marine systems [***Capone and Kiene*, 1988**]) (**Figures 2a and 2c**). According to a recent study by ***Alin and Johnson* [2007]** this ancient and deep tropical lake stores up to 4 km of sediment, containing a gigantic amount of organic matter, which is partially prone to remineralization at high deep water temperatures [***Sobek et al.*, 2009**] as encountered in Lake Tanganyika. The CH_4 'light' C isotopic ratio of −73 ‰ in deep water (**Figures 2a and 2c**) suggests that it is biologically produced, namely via carbon dioxide (CO_2) reduction or fermentation [***Whiticar et al.*, 1986**]. Typical $\delta^{13}C$ values produced by both processes in marine and fresh waters are −110 to −55 ‰ for CO_2 reduction and −70 to −50 ‰ for fermentation. Although Lake Tanganyika is a tectonic system, contribution of 'light' hydrocarbon gases (−58 to −50 ‰) originating from hydrothermal fluids [***Botz and Stoffers*, 1993**] did not impact the isotopic signature of water column CH_4.

[40] In both basins water column concentrations of dissolved CH_4 gradually declined upwards within deep anoxic layers and above in the mixolimnion, while intensely within the fairly narrow thermocline between 90 and 300 m (**Figures 2a and 2c**). The vertical profiles of CH_4 indicate

that (1) turbulent diffusion must lead to an upward flux of CH_4 from CH_4-rich deep water and (2) a sink for CH_4 exists at shallower depth compensating the upward flux. Significant vertical gradients in CH_4 concentrations were only identified in the anoxic zone, and did not extend into the oxic layer in the southern basin, suggesting that CH_4 must be substantially removed in anoxic water. Because of ample SO_4^{2-} concentrations in the stratified water column of Lake Tanganyika, we hypothesize that next to aerobic oxidation the anaerobic oxidation of CH_4 may play a role in the elimination of CH_4. According to ***Rudd* [1980]** no oxidative removal of CH_4 can be expected below the suboxic zone of Lake Tanganyika. However, one study has demonstrated that the anaerobic oxidation of CH_4 may act as a control mechanism of water column concentrations of CH_4 in freshwater [***Eller et al.*, 2005**]. For this reason, we have evaluated the importance of anaerobic and aerobic methanotrophy for CH_4 concentrations in Lake Tanganyika by means of a simplified one-dimensional model.

[41] We found that both in the deep water and in the thermocline, microenvironments geochemically suitable for the anaerobic oxidation of CH_4 existed with sufficiently high concentrations of both SO_4^{2-} and CH_4 [***Iversen and Jorgensen*, 1985**]. SO_4^{2-} is supplied intermittently to the CH_4-rich deep water by deep water renewal events, whereas in the thermocline turbulent diffusion supplies SO_4^{2-} from the mixolimnion and CH_4 from the deep water. This finding is strongly underscored by simulated rates of the anaerobic oxidation of CH_4, and simulated fluxes of CH_4, SO_4^{2-}, and HS^-, which also peaked in this depth range (**Figure 2d**).

[42] Sulphate is mainly supplied from river inflow [e.g., ***Kimbadi et al.*, 1999**; ***Langenberg et al.*, 2003**] and in-lake oxic and anoxic sulfur oxidation between ~150 to 300 m depth, as indicated by the existence of green nonsulphur bacteria in the lake's hypolimnion [***De Wever et al.*, 2005**]. Highest downward diffusive fluxes of SO_4^{2-} (~100 mol s^{-1}) occurred within the thermocline at ~200 m depth, and matched upward fluxes of HS^- (**Figure 9**). Hence, we concluded that HS^- concentrations were controlled by SO_4^{2-} reduction. Although thermophilic SO_4^{2-} reduction coupled to oxidation of organic matter was reported from sublacustrine hydrothermal sediments of Lake Tanganyika [***Elsgaard et al.*, 1994**], we assumed this process was potentially hampered in these depths due to relatively low SO_4^{2-} concentrations and mutual exclusion by methanogenesis [***Cappenberg*, 1974**; ***Lovley et al.*, 1982**].

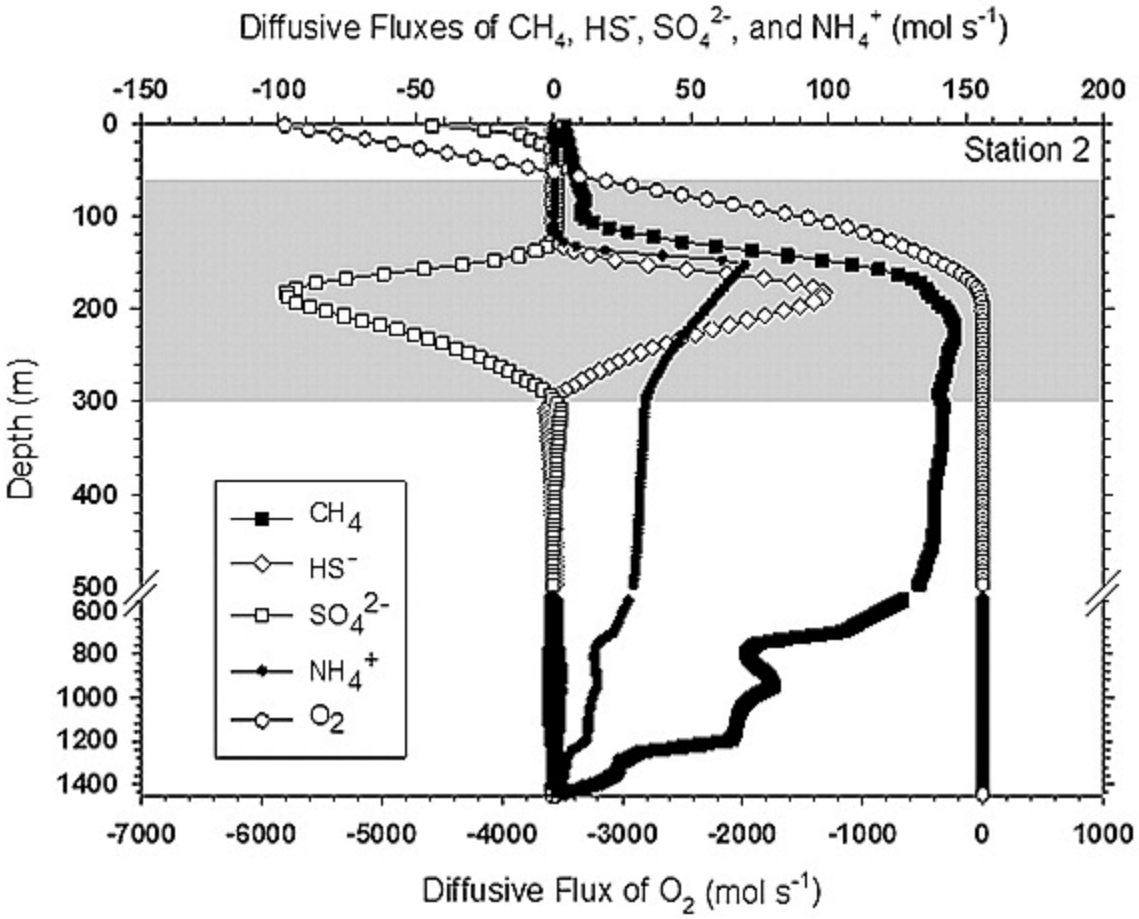

Figure 9

[Open in figure viewerPowerPoint]

Simulated diffusive fluxes (mol s^{-1}) of CH_4, NH_4^+, HS^-, and the electron acceptors SO_4^{2-} and O_2 for the anaerobic and aerobic oxidation of CH_4 versus depth. Negative values indicate downward and positive values upward fluxes. The thermocline zone is indicated by shading.

[43] The electron acceptor O_2, relevant for the aerobic oxidation of CH_4 ($CH_4 + 2O_2 \rightarrow CO_2 + 2H_2O$), is mainly supplied from the atmosphere. Oxygen concentrations decreased from 60 m downward and were zero at ~200 m depth in both basins (**Figures 2a and 2c**). Downward fluxes of oxygen were highly surpassing upward diffusion of CH_4, implying that the aerobic oxidation of CH_4 can be potentially very high in surface waters (**Figures 2d** and **9**). Hence, aerobic methanotrophy can occur until O_2 is depleted to zero, and it is the thermodynamically favorable process in the oxic and upper part of the suboxic zone [***Hazeu*, 1975**]. Estimated aerobic oxidations rates peaked at ~140 m depth, exactly where O_2 concentrations were already strongly depleted, as was previously described [***Rudd*, 1980**; ***Reeburgh et al.*, 1991**].

[44] According to simulations, ~35 km^3 yr^{-1} of water was exchanged by advective processes between the upper 90 m and the deep water below. The estimated deep water renewal rate was similar to the total annual river inflows. However, rivers have been shown to usually stratify at shallow depths and therefore cannot be the major source for this deep water renewal [***Verburg and Hecky*, 2009**]. Most probably, density plumes caused by differential cooling of water masses in shallower areas during the dry season are the cause for the deep water exchange. The lowest potential temperature in the vertical profiles was about 23.2°C. The difference in conductivity at 25°C between the surface and the deep water is only about 40–60 μS cm^{-1}, which corresponds to a density difference of <0.03 kg m^{-3}. At such high temperatures a difference of ~0.1°C is sufficient to compensate the stabilizing effect of the salinity differences between surface and deep water. Consequently, surface water masses that are cooled below 23°C can plunge to largest depths in Lake Tanganyika. Nearshore temperatures below 23°C were observed in three of four years during a measurement campaign at Mpulungu harbor [***Verburg and Hecky*, 2009**]. If the deep water renewal is indeed caused by such density plumes, small differences in the minimum temperature can have a large impact on both the volume and the intrusion depth of these plumes. Therefore, it is expected that the volume of deep water renewal as well as the depths of the resulting intrusions are highly variable from year to year. For example, observations from 1998 indicate the occurrence of a large plume at 400 m depth during the previous year. The estimated deep water renewal rate of ~35 km^3 yr^{-1} should be regarded as a long-term average rate. As mentioned above, the sinking water masses transport the oxidants O_2 and SO_4^{2-} from the surface layer to deeper waters.

[45] The model was able to adequately reproduce measured concentrations of CH_4, O_2, SO_4^{2-}, and HS^- in the southern basin (**Figure 2c**). In the anoxic deep, a net source of 6 g CH_4-C m^{-2} yr^{-1} was required to obtain the observed CH_4 concentrations. Furthermore, simulated concentrations of SO_4^{2-} and HS^- in the thermocline and below ~300 m depth could only be explained by assuming a slow transformation of SO_4^{2-} to HS^- with a residence time of SO_4^{2-} on the order of 300 years. We propose that the process responsible for this transformation is anaerobic oxidation of CH_4. The simulated depth distribution of the aerobic oxidation of CH_4 in the whole water column (**Figure 2d**) revealed highest rates at ~140 m depth under oxic/suboxic conditions, confirming the finding by ***Rudd* [1980]**. According to the model additional significant CH_4 removal is required at ~200 m depth under quasi anoxic conditions suggesting anaerobic CH_4 oxidation (**Figure 2d**). Moreover, the simulations suggested that the anaerobic oxidation of CH_4 took place within the whole anoxic deep, even though with a lower rate than in the thermocline. The reaction rate constants were roughly estimated to be 0.02 yr^{-1} (μM O_2)$^{-1}$ for the aerobic, and to 0.003 yr^{-1} (μM SO_4^{2-})$^{-1}$ and 0.0004 yr^{-1} (μM SO_4^{2-})$^{-1}$for the anaerobic elimination of CH_4 in the

thermocline and the deep water, respectively. Overall, according to the model, anaerobic and aerobic methane oxidation removed each about half of the CH_4 released from mineralization in the deep water. The simulated average residence time of CH_4 produced below 90 m depth was ~110 years (**Figure 6**).

[46] In the model, only a few percent of the CH_4 produced in the deep water were emitted to the atmosphere. However, simulated CH_4 concentrations in the surface layer were only 0.014 μM, whereas observed concentrations ranged between 0.01 and 10 μM. Therefore, it must be expected that CH_4 emissions to the atmosphere are higher than predicted by the model. A large number of observations would be required to calibrate a model that would aim at reproducing the seasonal variability of surface layer CH_4 concentrations, and could therefore give a reliable estimate of emissions to the atmosphere. The available data is insufficient for this purpose. Nevertheless, in order to arrive at an average concentration of 1 μM in the surface layer, an additional input of about 10 g C-CH_4 m^{-2} yr^{-1} had to be added to the model. Approximately half of this additional input would be oxidized aerobically, the other half would be emitted to the atmosphere. Potential sources of CH_4 to the surface layer could be CH_4, which is produced in nearshore shallow areas, especially near river inflows, and subsequently distributed horizontally, or CH_4 directly introduced by rivers [***Murase et al.*, 2005**; ***Schmid et al.*, 2007**].

[47] The isotopic enrichment of heavy carbon (^{13}C) in dissolved CH_4 served as an additional valuable evidence for biological CH_4 removal [***Barker and Fritz*, 1981**; ***Reeburgh et al.*, 1991**; ***Whiticar*, 1999**; ***Durisch-Kaiser et al.*, 2005**] and was compared to model calculations. We observed that microbial oxidation enforced a change in $\delta^{13}CH_4$ along upward CH_4 transport. In the narrow zone between 90 to 350 m depth, an isotopic enrichment by on average 23‰ (**Figures 2a and 2c**) was identified. Mixing processes as a reason for this isotopic imprint can be ruled out due to the lack of sufficient amounts of isotopically heavy CH_4 in these shallow depths. Furthermore, changes in CH_4 concentrations and in $\delta^{13}CH_4$ did not overlap depthwise (**Figures 2a and 2c**). This is explained by the low isotope fractionation factor for the anaerobic oxidation of CH_4 ($\varepsilon_C = 5$). A significant change in the C isotope ratio is first observed if ~80% of the CH_4 have been oxidized [***Whiticar*, 1999**].

[48] Isotopic analyses did not allow for distinguishing between aerobic and anaerobic processes. Hence, to constrain the role of both processes, we detected numerous single archaea and bacteria potentially involved in the oxidation of methane by using FISH [***Pernthaler et al.*, 2002**; ***Eller et al.*, 2001**]. Between 175 and 300 m depth, an enormously elevated abundance of archaea matched with pronounced changes in concentrations of CH_4, $\delta^{13}CH_4$, and calculated oxidation rates of CH_4 (**Figures 2c and 2d**). Abundances of ~0.6 to at most 33% archaea of 4′,6′-

diamidino-2-phenylindol (DAPI)-stained cells were detected in the thermocline of the northern basin. In the southern basin, highest numbers were located at around 200 m depth, perfectly coinciding with highest calculated rates of the anaerobic oxidation of CH_4 (**Figure 2d**). Archaea were also present in smaller amounts below ~350 m, aligning with simulations that predict anaerobic oxidation of CH_4 in the whole water column. We cannot exclude that increased numbers of archaea may also result from an elevated abundance of methanogens. However, the proper correlation ($R = 0.86$, $P < 0.0001$) of archaeal cell counts with simulated rates of the anaerobic oxidation of CH_4 suggested a dominant role of archaeal methanotrophs. Methanotrophs of aerobic physiology could also be located using FISH and specific probes for bacterial type I and II methanotrophs [***Eller et al.*, 2001**]. Highest abundances (up to 95% type I methanotrophs) occurred close to the top of the suboxic regime, confirming the pattern in calculated aerobic oxidation rates (**Figure 2d**) and a former study by ***Rudd* [1980]**.

[49] Empirical data and simulations provided several arguments for the assumption that the anaerobic oxidation of CH_4 is an important removal process for CH_4 in Lake Tanganyika today. First, model calculation allowed identifying a substantial deep water renewal process as a continuous mechanism supplying the electron acceptor SO_4^{2-} to the very deep. Second, between ~150 and 300 m depth downward fluxes of SO_4^{2-} matched upward fluxes of CH_4 and HS^- which is consistent with the anaerobic oxidation of CH_4 stoichiometry. Third, the overlap of archaeal numbers with calculated rates of the anaerobic oxidation of CH_4 validate the occurrence and importance of the anaerobic oxidation of CH_4. In conclusion, the available data support that anaerobic oxidation of CH_4 is an important mechanism controlling CH_4 removal in the deep water of Lake Tanganyika. Nevertheless, the vertical CH_4 profile could also be reproduced with an adapted version of the model without AOM. Ultimate proof of the importance of AOM will therefore require on one hand in situ rate measurements and biomarker analyses, and on the other hand cloning and sequencing of archaea present in the anoxic water column.

[50] It has been speculated that global warming may enforce stratification and that, as a consequence, the anoxic water mass will expand to shallower depths within the upcoming 100 years in Lake Tanganyika [***Verburg et al.*, 2003**; ***Verburg and Hecky*, 2009**; ***Cohen et al.*, 2006**]. We consider that this change could largely affect the vertical flux of important reactants in the anaerobic oxidation of CH_4, at least until the system has reached a new steady state. Hence, meanwhile the anaerobic oxidation of CH_4 will stay a major factor restraining CH_4 release to the atmosphere, however, over longer time periods an enforced stratification and higher minimal surface temperatures may impede vertical input of O_2 and SO_4^{2-} as well as deep water renewal. As a net result CH_4 may accumulate below the thermocline.

Acknowledgments

[51] We thank the whole crew of the R/V *Maman Benita* for logistical assistance during the research cruises, R. Illi for assisting laboratory analyses, L. Jarc for contributing to the development of the model, E. Deleersnijder for supplying bathymetry data, and two anonymous reviewers for their very helpful comments. This work was supported by internal Eawag funds. Isotopic measurements were possible due to a R'Equip grant from the Swiss National Science Foundation to Carsten J. Schubert.